Hyperuniformity and its generalizations

Salvatore Torquato

Department of Chemistry, Department of Physics, Princeton Center for Theoretical Science,
Program of Applied and Computational Mathematics, Princeton Institute for the Science and Technology of Materials,
Princeton University, Princeton, New Jersey 08544, USA

Disordered many-particle hyperuniform systems are exotic amorphous states of matter that lie between crystal and liquid: They are like perfect crystals in the way they suppress large-scale density fluctuations and yet are like liquids or glasses in that they are statistically isotropic with no Bragg peaks. These exotic states of matter play a vital role in a number of problems across the physical, mathematical as well as biological sciences and, because they are endowed with novel physical properties, have technological importance. Given the fundamental as well as practical importance of disordered hyperuniform systems elucidated thus far, it is natural to explore the generalizations of the hyperuniformity notion and its consequences. In this paper, we substantially broaden the hyperuniformity concept along four different directions. This includes generalizations to treat fluctuations in the interfacial area (one of the Minkowski functionals) in heterogeneous media and surface-area driven evolving microstructures, random scalar fields, divergence-free random vector fields, and statistically anisotropic many-particle systems and two-phase media. In all cases, the relevant mathematical underpinnings are formulated and illustrative calculations are provided. Interfacial-area fluctuations play a major role in characterizing the microstructure of two-phase systems (e.g., fluid-saturated porous media), physical properties that intimately depend on the geometry of the interface, and evolving two-phase microstructures that depend on interfacial energies (e.g., spinodal decomposition). In the instances of random vector fields and statistically anisotropic structures, we show that the standard definition of hyperuniformity must be generalized such that it accounts for the dependence of the relevant spectral functions on the direction in which the origin in Fourier space is approached (nonanalyticities at the origin). Using this analysis, we place some well-known energy spectra from the theory of isotropic turbulence in the context of this generalization of hyperuniformity. Among other results, we show that there exist many-particle ground-state configurations in which directional hyperuniformity imparts exotic anisotropic physical properties (e.g., elastic, optical, and acoustic characteristics) to these states of matter. Such tunability could have technological relevance for manipulating light and sound waves in ways heretofore not thought possible. We show that disordered many-particle systems that respond to external fields (e.g., magnetic and electric fields) are a natural class of materials to look for directional hyperuniformity. The generalizations of hyperuniformity introduced here provide theoreticians and experimentalists new avenues to understand a very broad range of phenomena across a variety of fields through the hyperuniformity "lens."

I. INTRODUCTION

The characterization of density fluctuations in many-body systems is a problem of great fundamental interest in the physical, mathematical, and biological sciences [1–15]. The anomalous suppression of density fluctuations at very long wavelengths is central to the hyperuniformity concept, whose broad importance for condensed matter physics and materials science was brought to the fore only about a decade ago in a study that focused on fundamental theoretical aspects, including how it provides a unified means to classify and categorize crystals, quasicrystals, and special disordered point configurations [16]. Hyperuniform systems are poised at an exotic critical point in which the direct correlation function, defined via the Ornstein-Zernike relation [17], is long-ranged [16], in diametric contrast to standard thermal and magnetic critical points in which the total correlation function is long-ranged [1–4]. Roughly speaking, a hyperuniform many-particle system in d-dimensional Euclidean space $\mathbb{R}^d$ is one in which (normalized) density fluctuations are completely suppressed at very large length scales, implying that the structure factor $S(\mathbf{k})$ tends to zero as the wave number $k \equiv |\mathbf{k}|$

tends to zero; i.e.,

$$\lim_{|\mathbf{k}| \to 0} S(\mathbf{k}) = 0. \tag{1}$$

Equivalently, it is one in which the number variance $\sigma_N^2(R)$ of particles within a spherical observation window of radius R grows more slowly than the window volume in the large-R limit, i.e., slower than R^d. Typical disordered systems, such as liquids and structural glasses, have the standard volume scaling; that is, $\sigma_N^2(R) \sim R^d$. By contrast, all perfect crystals and quasicrystals are hyperuniform with the surface-area scaling $\sigma_N^2(R) \sim R^{d-1}$. Surprisingly, there are a special class of disordered particle configurations that have the same asymptotic behavior as crystals. There are hyperuniform scalings other than surface-area growth. When the structure factor goes to zero in the limit $|\mathbf{k}| \to 0$ with the power-law form

$$S(\mathbf{k}) \sim |\mathbf{k}|^\alpha, \tag{2}$$

where $\alpha > 0$, the number variance has the following large-R asymptotic scaling [16,18,19]:

$$\sigma_N^2(R) \sim \begin{cases} R^{d-1}, & \alpha > 1, \\ R^{d-1}\ln R, & \alpha = 1, \\ R^{d-\alpha}, & 0 < \alpha < 1. \end{cases} \quad (R \to \infty). \quad (3)$$

The exponent α can take any positive real value (including $+\infty$ for a crystal and "stealthy" disordered patterns), the magnitude of which is a rough measure of short-range order in the particular hyperuniform system; see Ref. [20] and references therein for explicit examples of systems with various values of α.

Disordered hyperuniform systems are exotic states of matter that lie between a crystal and liquid: They are like perfect crystals in the way they suppress large-scale density fluctuations and yet are like liquids or glasses in that they are statistically isotropic with no Bragg peaks and hence have no long-range order. In this sense, they can have a *hidden order on large length scales* (see Fig. 2 of Ref. [20] for a vivid example) and, because of their hybrid nature, are endowed with novel physical properties, as described below. Figure 1 shows a typical scattering pattern for a crystal and another for a "stealthy" disordered hyperuniform one in which there is a circular region around the origin in which there is no scattering and diffuse scattering outside this "exclusion" zone [21,22], highly unusual for an amorphous material.

We knew only a few examples of *disordered* hyperuniform systems (also known as "superhomogeneous" patterns) about a decade ago [16,23,24]. We now know that these exotic states of matter can exist as *equilibrium* and *nonequilibrium* phases of both the classical and the quantum-mechanical varieties. Examples include "stealthy" disordered ground states [20–22,25,26], maximally random jammed particle packings [27–30], jammed athermal granular media [31], jammed thermal colloidal packings [32–34], dynamical processes in ultracold atoms [35], disordered networks with large photonic band gaps [36], driven nonequilibrium systems [37–42], avian photoreceptor patterns [43], geometry of neuronal tracts [44], immune system receptors [45], certain quantum ground states (both fermionic and bosonic) [46,47], high-density transparent materials [48], and wave dynamics in disordered potentials [49]. Hyperuniformity has pointed to new correlation functions from which one can extract relevant growing length scales as a function of temperature as a liquid is supercooled below its glass transition temperature [50,51], a problem of great interest in glass physics [14,52–56]. Remarkably, the one-dimensional point patterns derived from the nontrivial zeros of the Riemann zeta function [57] and the eigenvalues of random Hermitian matrices [58] are disordered and hyperuniform.

A variety of groups have recently fabricated disordered hyperuniform materials at the micro- and nanoscales for various photonic applications [59–61], surface-enhanced Raman spectroscopy [62], realization of a terahertz quantum cascade laser [63], and self-assembly of diblock copolymers [64]. Moreover, it was shown that the electronic band gap of amorphous silicon widens as it tends toward a hyperuniform state [65]. Recent x-ray scattering measurements indicate that amorphous-silicon samples can be made to be nearly hyperuniform [66].
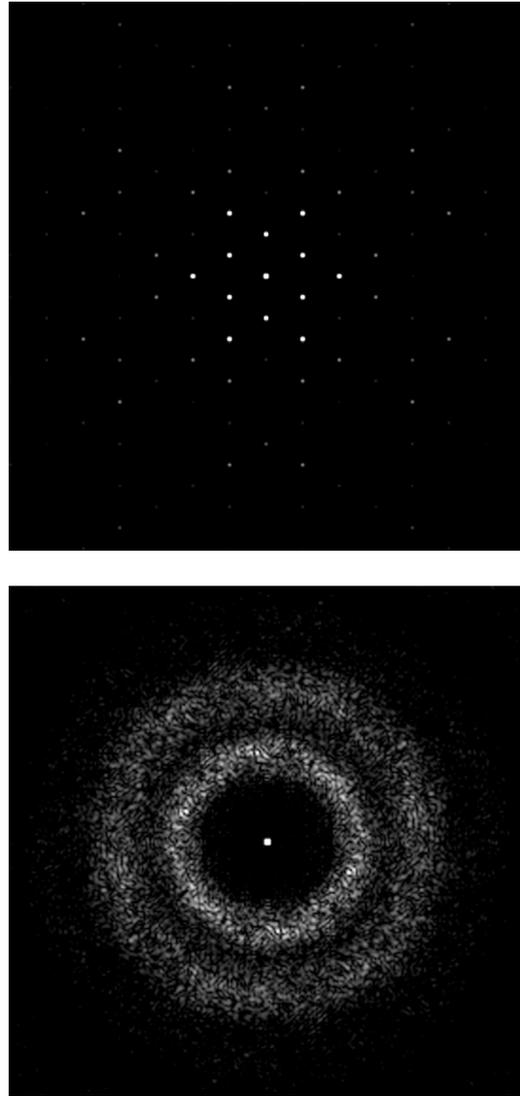

FIG. 1. (Top) Scattering pattern for a crystal. (Bottom) Scattering pattern for a disordered "stealthy" hyperuniform material [21,22]. Notice that, apart from forward scattering, there is a circular region around the origin in which there is no scattering, a highly exotic situation for an amorphous state of matter.

The hyperuniformity concept was generalized to the case of heterogeneous materials [18], i.e., materials consisting of two or more phases [67]. Heterogeneous materials abound in nature and synthetic situations. Examples include composite and porous media, biological media (e.g., plant and animal tissue), foams, polymer blends, suspensions, granular media, cellular solids, and colloids [68]. In the case of two-phase media (defined more precisely in Sec. II), one relevant fluctuating quantity is the local phase volume fraction within a window. The simplest characterization of such fluctuations is the local volume-fraction variance $\sigma_V^2(R)$ associated with a d-dimensional spherical window of radius R [68–71]. It was demonstrated that the hyperuniformity condition in the context of volume-fraction fluctuations in a two-phase heterogeneous system is one in which the variance $\sigma_V^2(R)$ for large R goes to zero more rapidly than the inverse of the window volume

[18], i.e., faster than R^{-d}, which is equivalent to the following condition on the relevant spectral density $\tilde{\chi}_V(\mathbf{k})$ (defined in Sec. II):

$$\lim_{|\mathbf{k}|\to 0} \tilde{\chi}_V(\mathbf{k}) = 0. \tag{4}$$

This generalization of the hyperuniformity concept has been fruitfully applied to characterize a variety of disordered two-phase systems [28,34,72–74] and the rational design of digitized hyperuniform two-phase media with tunable disorder [75]. As in the case of hyperuniform point configurations [16,18,19], it is easily shown that three different scaling regimes arise in the case of hyperuniform two-phase systems when the spectral density goes to zero with the power-law form $\tilde{\chi}_V(\mathbf{k}) \sim |\mathbf{k}|^\alpha$:

$$\sigma_V^2(R) \sim \begin{cases} R^{-(d+1)}, & \alpha > 1, \\ R^{-(d+1)}\ln R, & \alpha = 1, \qquad (R \to \infty). \\ R^{-(d+\alpha)}, & 0 < \alpha < 1, \end{cases} \tag{5}$$

Given the fundamental as well as practical importance of disordered hyperuniform systems elucidated thus far, it is natural to explore further generalizations of the hyperuniformity notion and its consequences. In this paper, we extend the hyperuniformity concept in a variety of different directions. Before doing so, we make some remarks about hyperuniformity in two-phase systems in which one phase is a sphere packing (Sec. III). We then introduce the notion of hyperuniformity as it concerns local fluctuations in the interfacial area in disordered two-phase media and apply the mathematical formulation to sphere packings (Sec. IV). We demonstrate that surface-area fluctuations are considerably more sensitive microstructural measures than volume-fraction fluctuations and hence provide a more powerful approach to understand hyperuniformity in two-phase systems. Subsequently, we extend the hyperuniformity concept to random scalar fields (Sec. V). Such phenomena are ubiquitous and include, but are not limited to, concentration and temperature fields in heterogeneous media and turbulent flows, laser speckle patterns, and temperature fluctuations associated with the cosmic microwave background. Among other results, we show how a random scalar field can inherit the hyperuniformity property from an underlying hyperuniform point process. We also note that the analysis for continuous random fields is trivially extended to discrete cases derived from experimental images or computer-simulation studies. We then generalize the hyperuniformity formalism to treat random vector fields and find that this extension requires one to broaden the definition of hyperuniformity to account for the dependence of the relevant spectral tensor function on the direction in which the origin is approached (Sec. VI). Mathematically, this means that the directional-dependent spectral tensor associated with a hyperuniform vector field is nonanalytic at the origin. This is to be contrasted with previous definitions of hyperuniformity, which assumed that the way in which the origin in Fourier space (scattering pattern) is approached is independent of direction. Generalizing the definition of hyperuniformity to account for directionality provides completely new and potentially exciting avenues for theoretical and experimental work, including the possibility to design random vector fields

with targeted hyperuniform spectra. Among other results, we reinterpret and analyze well-known turbulent energy spectra in the context of this generalization of hyperuniformity. Subsequently, the notion of directional hyperuniformity is proposed in the context of many-particle systems and heterogeneous media that are statistically anisotropic (Sec. VII). Here we show that directionality in Fourier space can again play a pivotal role. In particular, directional hyperuniformity imparts exotic anisotropic physical properties (e.g., elastic, optical and acoustic characteristics) to these states of matter. Finally, we offer concluding remarks and a discussion (Sec. VIII).

II. DEFINITIONS AND BACKGROUND

A. Point configurations

Consider N points with configuration $\mathbf{r}^N \equiv \mathbf{r}_1, \mathbf{r}_2, \ldots, \mathbf{r}_N$ in a large region $\mathcal{V}$ of volume V in d-dimensional Euclidean space $\mathbb{R}^d$. Any single-point configuration is specified by its *microscopic density* $n(\mathbf{r})$ at position $\mathbf{r}$, which is a random variable defined by

$$n(\mathbf{r}) = \sum_{j=1}^N \delta(\mathbf{r} - \mathbf{r}_j), \tag{6}$$

where $\delta(\mathbf{r})$ is a d-dimensional Dirac δ function. The point process is statistically characterized by the *specific* probability density function $P_N(\mathbf{r}^N)$, where $P_N(\mathbf{r}^N)d\mathbf{r}^N$ gives the probability of finding point 1 in volume element $d\mathbf{r}_1$ about $\mathbf{r}_1$, point 2 in volume element $d\mathbf{r}_2$ about $\mathbf{r}_2, \ldots$, and point N in volume element $d\mathbf{r}_N$ about $\mathbf{r}_N$. Thus, $P_N(\mathbf{r}^N)$ normalizes to unity and $d\mathbf{r}^N \equiv d\mathbf{r}_1 d\mathbf{r}_2 \cdots d\mathbf{r}_N$ represents the (Nd)-dimensional volume element. The ensemble average of any function $f(\mathbf{r}^N)$ that depends on the point configuration $\mathbf{r}^N$ is given by

$$\langle f(\mathbf{r}^N) \rangle = \int_{\mathcal{V}} \int_{\mathcal{V}} \cdots \int_{\mathcal{V}} f(\mathbf{r}^N) P_N(\mathbf{r}^N) d\mathbf{r}^N. \tag{7}$$

The reduced *generic* density function $\rho_n(\mathbf{r}^n)$ $(n < N)$, defined as

$$\rho_n(\mathbf{r}^n) = \frac{N!}{(N-n)!} \int_V \cdots \int_V P_N(\mathbf{r}^N) d\mathbf{r}^{N-n}, \tag{8}$$

where $d\mathbf{r}^{N-n} \equiv d\mathbf{r}_{n+1} d\mathbf{r}_{n+2} \cdots d\mathbf{r}_N$. The quantity $\rho_n(\mathbf{r}^n) d\mathbf{r}^n$ is proportional to the probability of finding *any* n particles $(n \leqslant N)$ with configuration $\mathbf{r}^n$ in volume element $d\mathbf{r}^n$.

For statistically homogeneous media, $\rho_n(\mathbf{r}^n)$ is translationally invariant and hence depends only on the relative displacements, say with respect to $\mathbf{r}_1$,

$$\rho_n(\mathbf{r}^n) = \rho_n(\mathbf{r}_{12}, \mathbf{r}_{13}, \ldots, \mathbf{r}_{1n}), \tag{9}$$

where $\mathbf{r}_{ij} = \mathbf{r}_j - \mathbf{r}_i$. The one-particle function ρ_1 is just equal to the constant *number density* of particles ρ; i.e.,

$$\rho_1(\mathbf{r}_1) = \rho \equiv \lim_{N,V\to\infty} \frac{N}{V}. \tag{10}$$

This limit is referred to as the *thermodynamic limit*. It is convenient to define the so-called *n-particle correlation function*,

$$g_n(\mathbf{r}^n) = \frac{\rho_n(\mathbf{r}^n)}{\rho^n}. \tag{11}$$

In the absence of long-range order and when the particles are mutually far from one another (i.e., $r_{ij} = |\mathbf{r}_{ij}| \to \infty$, $1 \leqslant i < j \leqslant N$), $\rho_n(\mathbf{r}^n) \to \rho^n$, and $g_n(\mathbf{r}^n) \to 1$.

The important two-particle quantity

$$g_2(\mathbf{r}_{12}) = \frac{\rho_2(\mathbf{r}_{12})}{\rho^2} \qquad (12)$$

is usually referred to as the *pair correlation function*. The *total correlation function* $h(\mathbf{r}_{12})$ is defined as

$$h(\mathbf{r}_{12}) = g_2(\mathbf{r}_{12}) - 1, \qquad (13)$$

which is trivially related to the autocovariance function associated with the random variable (6), i.e,

$$\frac{1}{\rho}\langle[n(\mathbf{x}) - \rho][n(\mathbf{x}+\mathbf{r}) - \rho]\rangle = \delta(\mathbf{r}) + \rho h(\mathbf{r}), \qquad (14)$$

where we have invoked statistical homogeneity.

Spectral representations of direct-space pair statistics of various types are central to the hyperuniformity concept. We use the following definition of the Fourier transform of some function $f(\mathbf{r})$, which can represent a *tensor of arbitrary rank* and depends on the vector $\mathbf{r}$ in $\mathbb{R}^d$,

$$\tilde{f}(\mathbf{k}) = \int_{\mathbb{R}^d} f(\mathbf{r}) \exp[-i(\mathbf{k}\cdot\mathbf{r})]d\mathbf{r}, \qquad (15)$$

where $\mathbf{k}$ is a wave vector. When it is well defined, the corresponding inverse Fourier transform is given by

$$f(\mathbf{r}) = \left(\frac{1}{2\pi}\right)^d \int_{\mathbb{R}^d} \tilde{f}(\mathbf{k}) \exp[i(\mathbf{k}\cdot\mathbf{r})]d\mathbf{k}. \qquad (16)$$

If f is a radial function, i.e., depends on the modulus $r = |\mathbf{r}|$ of the vector $\mathbf{r}$, its Fourier transform is given by

$$\tilde{f}(k) = (2\pi)^{\frac{d}{2}} \int_0^\infty r^{d-1} f(r) \frac{J_{(d/2)-1}(kr)}{(kr)^{(d/2)-1}} \, dr, \qquad (17)$$

where $k = |\mathbf{k}|$ is wave number or modulus of the wave vector $\mathbf{k}$ and $J_\nu(x)$ is the Bessel function of order ν. The inverse transform of $\tilde{f}(k)$ is given by

$$f(r) = \frac{1}{(2\pi)^{\frac{d}{2}}} \int_0^\infty k^{d-1} \tilde{f}(k) \frac{J_{(d/2)-1}(kr)}{(kr)^{(d/2)-1}} dk. \qquad (18)$$

We recall the first several terms in the series expansion of $J_\nu(x)$ about $x = 0$:

$$J_\nu(x) = \frac{(x/2)^\nu}{\Gamma(\nu+1)} - \frac{(x/2)^{\nu+2}}{\Gamma(\nu+2)} + \frac{(x/2)^{\nu+4}}{2\Gamma(\nu+3)} - \mathcal{O}(x^{\nu+6}), \qquad (19)$$

which we apply later in the article.

The non-negative structure factor $S(\mathbf{k})$ is the Fourier transform of the autocovariance function (14) and is trivially related to $\tilde{h}(\mathbf{k})$, which is the Fourier transform of the total correlation function $h(\mathbf{r})$:

$$S(\mathbf{k}) = 1 + \rho\tilde{h}(\mathbf{k}). \qquad (20)$$

The structure factor is proportional to the scattering intensity. It is useful to recall the relationship between the local number variance $\sigma_N^2(R)$ associated with a spherical window of radius

R for a point configuration [16],

$$\sigma_N^2(R) = \rho v_1(R)\left[1 + \rho \int_{\mathbb{R}^d} h(\mathbf{r})\alpha(r;R)d\mathbf{r}\right]$$
$$= \rho v_1(R)\left[\frac{1}{(2\pi)^d} \int_{\mathbb{R}^d} S(\mathbf{k})\tilde{\alpha}(k;R)d\mathbf{k}\right], \qquad (21)$$

where

$$v_1(R) = \frac{\pi^{d/2}R^d}{\Gamma(1+d/2)} \qquad (22)$$

is the volume of a d-dimensional sphere of radius R, and $\alpha(r;R)$ is the *scaled intersection volume*, the ratio of the intersection volume of two spherical windows of radius R whose centers are separated by a distance r to the volume of a spherical window, known analytically in any space dimension [68,76]. Its Fourier transform is given by

$$\tilde{\alpha}(k;R) = 2^d \pi^{d/2}\Gamma(1+d/2)\frac{[J_{d/2}(kR)]^2}{k^d}, \qquad (23)$$

which clearly is a non-negative function. Here $J_\nu(x)$ is the Bessel function of order ν.

The hyperuniformity condition (1) defined through the structure factor and relation (21) implies that the number variance $\sigma_N^2(R)$ grows more slowly than R^d for large R. Observe that hyperuniformity requirement (1) dictates that the volume integral of $\rho h(\mathbf{r})$ over all space is exactly equal to -1, i.e.,

$$\rho \int_{\mathbb{R}^d} h(\mathbf{r})d\mathbf{r} = -1, \qquad (24)$$

which can be thought of as a sum rule. *Stealthy* configurations are those in which the structure factor $S(\mathbf{k})$ is exactly zero for a subset of wave vectors, meaning that they completely suppress single scattering of incident radiation for those wave vectors. *Stealthy hyperuniform* patterns [20–22] are a subclass of hyperuniform systems in which $S(\mathbf{k})$ is zero for a range of wave vectors around the origin; i.e.,

$$S(\mathbf{k}) = 0 \quad \text{for } 0 \leqslant |\mathbf{k}| \leqslant K, \qquad (25)$$

where K is some positive number. An example of a disordered stealthy and hyperuniform scattering pattern is shown in the bottom panel of Fig. 1.

B. Two-phase media

A two-phase random medium is a domain of space $\mathcal{V} \subseteq \mathbb{R}^d$ of volume V that is partitioned into two disjoint regions: a phase 1 region $\mathcal{V}_1$ and a phase 2 region $\mathcal{V}_2$ such that $\mathcal{V}_1 \cup \mathcal{V}_1 = \mathcal{V}$ [68]. Denote by $\partial\mathcal{V}$ the interface between $\mathcal{V}_1$ and $\mathcal{V}_2$.

1. Phase statistics

The phase indicator function $\mathcal{I}^{(i)}(\mathbf{x})$ for a given realization is defined as

$$\mathcal{I}^{(i)}(\mathbf{x}) = \begin{cases} 1, & \mathbf{x} \in \mathcal{V}_i, \\ 0, & \mathbf{x} \notin \mathcal{V}_i. \end{cases} \qquad (26)$$

The one-point correlation function $S_1^{(i)}(\mathbf{x}) = \langle\mathcal{I}^{(i)}(\mathbf{x})\rangle$ (where angular brackets indicate an ensemble average) is

independent of position $\mathbf{x}$ for statistically homogeneous media, namely, the constant phase volume fraction; i.e.,

$$\phi_i = \langle \mathcal{I}^{(i)}(\mathbf{x}) \rangle. \tag{27}$$

The two-point correlation function is defined as $S_2^{(i)}(\mathbf{x}_1, \mathbf{x}_2) = \langle \mathcal{I}^{(i)}(\mathbf{x}_1) \mathcal{I}^{(i)}(\mathbf{x}_2) \rangle$. This function is the probability of finding two points $\mathbf{x}_1$ and $\mathbf{x}_2$ in phase i and, for homogeneous media, depends only on the relative displacement vector $\mathbf{r} \equiv \mathbf{x}_2 - \mathbf{x}_1$ and hence $S_2^{(i)}(\mathbf{x}_1, \mathbf{x}_2) = S_2^{(i)}(\mathbf{r})$. The autocovariance function $\chi_V(\mathbf{r})$ associated with the random variable $\mathcal{I}^{(i)}(\mathbf{x})$ is given by

$$\chi_V(\mathbf{r}) \equiv S_2^{(1)}(\mathbf{r}) - \phi_1^2 = S_2^{(2)}(\mathbf{r}) - \phi_2^2. \tag{28}$$

The non-negative spectral density $\tilde{\chi}_V(\mathbf{k})$, which can be obtained from scattering experiments [77,78], is the Fourier transform of $\chi_V(\mathbf{r})$. Higher-order versions of these correlation functions [68,79,80] (not considered here) arise in rigorous bounds and exact expressions for effective transport [68,81–88], elastic [68,83,85,86,89] and electromagnetic [90] properties of two-phase media.

It is known that the volume-fraction variance $\sigma_V^2(R)$ within a d-dimensional spherical window of radius R can be expressed in terms of the autocovariance function $\chi_V(\mathbf{r})$ [69] or of the spectral density $\tilde{\chi}_V(\mathbf{k})$,

$$\sigma_V^2(R) = \frac{1}{v_1(R)} \int_{\mathbb{R}^d} \chi_V(\mathbf{r}) \alpha(r; R) d\mathbf{r}$$
$$= \frac{1}{v_1(R)(2\pi)^d} \int_{\mathbb{R}^d} \tilde{\chi}_V(\mathbf{k}) \tilde{\alpha}(k; R) d\mathbf{k}, \tag{29}$$

where, as in relation (21), $\alpha(r; R)$ is the scaled intersection volume of two spherical windows, and $\tilde{\alpha}(k; R)$ is its Fourier transform. The hyperuniformity requirement (4) dictates that the autocovariance function $\chi_V(\mathbf{r})$ exhibits both positive and negative correlations such that its volume integral over all space is exactly zero, i.e.,

$$\int_{\mathbb{R}^d} \chi_V(\mathbf{r}) d\mathbf{r} = 0, \tag{30}$$

which can be regarded to be a sum rule.

We note in passing that realizability conditions for the existence of hyperuniform autocovariances and spectral densities of general two-phase media have recently been explored [91]. These conditions restrict the possible class of functional forms that can be hyperuniform.

2. Interfacial statistics

The interface between the phases of a realization of a two-phase medium is generally known probabilistically and is characterized by the interface indicator function $\mathcal{M}(\mathbf{x})$ [68], defined as

$$\mathcal{M}(\mathbf{x}) = |\nabla \mathcal{I}^{(1)}(\mathbf{x})| = |\nabla \mathcal{I}^{(2)}(\mathbf{x})|, \tag{31}$$

and therefore is a *generalized* function that is nonzero when $\mathbf{x}$ is on the interface. The specific surface s (interface area per unit volume) is a one-point correlation given by the expectation of $\mathcal{M}(\mathbf{x})$,

$$s = \langle \mathcal{M}(\mathbf{x}) \rangle, \tag{32}$$

where, because of the assumption of statistical homogeneity, s is independent of the position $\mathbf{x}$.

One can define a variety of higher-order surface correlation functions [68], but for our purposes in this paper, we restrict ourselves to the following two-point correlation function,

$$F_{ss}(\mathbf{r}) = \langle \mathcal{M}(\mathbf{x}) \mathcal{M}(\mathbf{x} + \mathbf{r}) \rangle, \tag{33}$$

which is called the *surface-surface* correlation function. Note the definition (33) invokes the statistical homogeneity of the process. The surface-surface correlation function arises in rigorous bounds on the effective rate constants for diffusion-controlled reactions [92,93] and fluid permeability [92,94] of fluid-saturated porous media. The autocovariance associated with the random variable $\mathcal{M}$ for homogeneous media is given by

$$\chi_s(\mathbf{r}) = F_{ss}(\mathbf{r}) - s^2, \tag{34}$$

which, unlike the dimensionless autocovariance $\chi_V(\mathbf{r})$, has dimensions of inverse of length squared, independent of the dimension d. The non-negative spectral density $\tilde{\chi}_s(\mathbf{k})$ is the Fourier transform of $\chi_s(\mathbf{r})$, when it exists.

III. SOME REMARKS ABOUT TWO-POINT STATISTICS AND HYPERUNIFORM SPHERE PACKINGS

Here we collect various known results scattered throughout the literature concerning the autocovariance function $\chi_V(\mathbf{r})$ and spectral density $\tilde{\chi}_V(\mathbf{k})$ for two-phase media in $\mathbb{R}^d$ in which one phase is a sphere packing in order to compare them to corresponding results for the surface-surface correlation function and the generalization of hyperuniformity to surface-area fluctuations introduced in the subsequent section.

A particle packing is a configuration of nonoverlapping (i.e., hard) particles in $\mathbb{R}^d$. For statistically homogeneous packings of congruent spheres of radius a in $\mathbb{R}^d$ at number density ρ, the two-point probability function $S_2(\mathbf{r})$ of the particle (sphere) phase is known exactly in terms of the pair correlation function [68,95]; specifically,

$$\chi_V(\mathbf{r}) = \rho m_v(r; a) \otimes m_v(r; a) + \rho^2 m_v(r; a) \otimes m_v(r; a) \otimes h(\mathbf{r})$$
$$= \rho v_2^{int}(r; a) + \rho^2 v_2^{int}(r; a) \otimes h(\mathbf{r}), \tag{35}$$

where

$$m_v(r; a) = \Theta(a - r) = \begin{cases} 1, & r \leqslant a, \\ 0, & r > a, \end{cases} \tag{36}$$

is a spherical particle indicator function [96]. $\Theta(x)$ is the Heaviside step function, and $v_2^{int}(r; a) = v_1(a)\alpha(r; a)$ is the intersection volume of two spheres of radius a whose centers are separated by a distance r, where $v_1(a)$ and $\alpha(r; a)$ are defined as in (29), and $\otimes$ denotes the convolution of two functions $F(\mathbf{r})$ and $G(\mathbf{r})$:

$$F(\mathbf{r}) \otimes G(\mathbf{r}) = \int_{\mathbb{R}^d} F(\mathbf{x}) G(\mathbf{r} - \mathbf{x}) d\mathbf{x}. \tag{37}$$

Fourier transformation of (35) gives the spectral density in terms of the structure factor [18,68,95],

$$\tilde{\chi}_V(\mathbf{k}) = \rho \tilde{m}^2(k; a) + \rho^2 \tilde{m}^2(k; a) \tilde{h}(\mathbf{k})$$
$$= \rho \tilde{m}^2(k; a) S(\mathbf{k})$$
$$= \phi \tilde{\alpha}(k; a) S(\mathbf{k}), \tag{38}$$

where

$$\tilde{\alpha}(k;a) = \frac{1}{v_1(a)} \tilde{m}^2(k;a) = \frac{1}{v_1(a)} \left(\frac{2\pi a}{k} \right)^d J_{d/2}^2(ka) \quad (39)$$

and

$$\phi = \rho v_1(a) \quad (40)$$

is the *packing fraction*.

Using relation (38), it follows that the hyperuniformity of a sphere packing can only arise if the underlying point configuration (sphere centers) is itself hyperuniform, i.e., $\tilde{\chi}_V(\mathbf{k})$ inherits the hyperuniformity property (4) only through the structure factor, not $\tilde{\alpha}(k;a)$; see Ref. [91] for more details. The stealthiness property, i.e., no scattering at some finite subset of wave vectors (Sec. II A), is a bit more subtle. Relation (38) dictates that $\tilde{\chi}_V(\mathbf{k})$ is zero at those wave vectors, where $S(\mathbf{k})$ is zero as well as at the zeros of the function $\tilde{\alpha}(k;a)$, which is determined by the zeros of the Bessel function $J_{d/2}(ka)$. The function $\tilde{\chi}_V(\mathbf{k})$ will be zero at all of the zeros of $\tilde{\alpha}(k;a)$ for any disordered packing free of any Dirac delta functions (Bragg peaks), hyperuniform or not.

These results for the pair statistics in direct and Fourier spaces have been generalized to the case of impenetrable spheres with a size distribution at overall number density ρ [68,97]. The Supplemental Material describes these equations as they concern hyperuniformity [98].

IV. INTERFACIAL AREA FLUCTUATIONS AND HYPERUNIFORMITY

Here we introduce the idea of hyperuniformity associated with local fluctuations in the interfacial area of two-phase media in $\mathbb{R}^d$ and derive the relevant formulas. This generalization provides new tools to analyze a variety of phenomena that occur in physical and biological systems in which interfaces play a dominant role. For example, the geometry of the interface in a fluid-saturated porous medium is crucial in determining the fluid permeability [92,94] and trapping rate [92,93] associated with diffusion and reaction in such systems. Another striking class of examples includes surface-energy driven coarsening phenomena, such as those that occur in spinodal decomposition and morphogenesis [99,100].

A. Local specific-surface fluctuations

While the global specific surface defined by (32) is a fixed constant, the specific surface on a local scale determined by an observation window clearly fluctuates, as in the case of the local phase volume fraction. Here we derive an explicit expression for the variance associated with the local specific surface and the corresponding hyperuniformity condition. For simplicity, we consider a d-dimensional spherical window of radius R centered at position $\mathbf{x}_0$ (see Fig. 2) for statistically homogeneous two-phase media. The associated *local dimensionless specific surface* $\tau_s(\mathbf{x}_0;R)$ within a window of radius R centered at position $\mathbf{x}_0$ is specified explicitly by

$$\tau_s(\mathbf{x}_0;R) = \frac{1}{s v_1(R)} \int \mathcal{M}(\mathbf{x}) w(\mathbf{x} - \mathbf{x}_0; R) d\mathbf{x}, \quad (41)$$
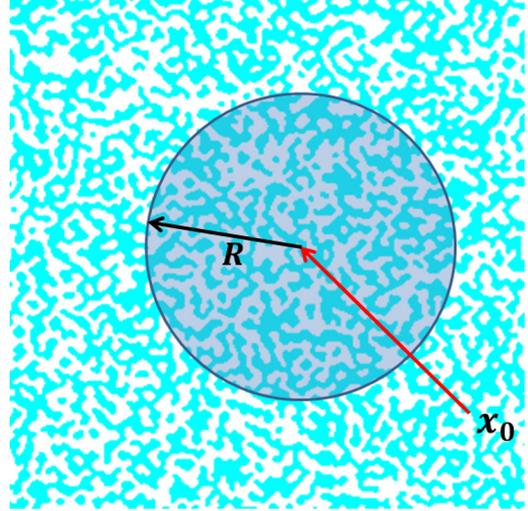

FIG. 2. A schematic indicating a circular observation window of radius R that is centered at position $\mathbf{x}_0$ in a disordered two-phase medium; one phase is depicted as a blue (darker) region and the other phase as a white region. The phase volume fractions or interfacial area within the window will fluctuate as the window position $\mathbf{x}_0$ is varied.

where $v_1(R)$ is given by (22), $\mathcal{M}(\mathbf{x})$ is the interface indicator function defined by (31), s is the specific surface given by (32), and w is the corresponding window indicator function defined by

$$w(\mathbf{r};R) = \begin{cases} 1, & |\mathbf{r}| \leqslant R, \\ 0, & |\mathbf{r}| > R. \end{cases} \quad (42)$$

Notice that in the limit $R \to \infty$, the dimensionless random variable $\tau_s(\mathbf{x}_0;R)$ tends to unity. The variance $\sigma_S^2(R)$ associated with fluctuations in dimensionless specific surface is defined by

$$\sigma_s^2(R) \equiv \langle \tau_s^2(\mathbf{x}_0;R) \rangle - \langle \tau_s(\mathbf{x}_0;R) \rangle^2$$
$$= \langle \tau_s^2(\mathbf{x}_0;R) \rangle - 1, \quad (43)$$

where we have used the fact that the ensemble average $\langle \tau_s(\mathbf{x}_0;R) \rangle = 1$, which is independent of the window position $\mathbf{x}_0$ because the system is statistically homogeneous.

Substitution of (41) into (43) yields

$$\sigma_s^2(R) = \frac{1}{s^2 v_1^2(R)} \left[\int F_{ss}(\mathbf{r}) w(\mathbf{x}_1 - \mathbf{x}_0; R) \right.$$
$$\left. \times w(\mathbf{x}_2 - \mathbf{x}_0; R) d\mathbf{x}_1 d\mathbf{x}_2 \right] - 1, \quad (44)$$

where $\mathbf{r} = \mathbf{x}_2 - \mathbf{x}_1$. Using the definition of the scaled intersection volume of two windows of radius R,

$$\alpha(r;R) = \frac{1}{v_1(R)} \int_{\mathbb{R}^d} w(\mathbf{x}_1 - \mathbf{x}_0; R) w(\mathbf{x}_2 - \mathbf{x}_0; R) d\mathbf{x}_0, \quad (45)$$

and the identity [16]

$$\frac{1}{v_1(R)} \int_{\mathbb{R}^d} \alpha(r;R) d\mathbf{r} = 1 \quad (46)$$

leads to the desired relation for the local specific-surface variance,

$$\sigma_s^2(R) = \frac{1}{s^2 v_1(R)} \int_{\mathbb{R}^d} \chi_s(\mathbf{r}) \alpha(r; R) d\mathbf{r}, \quad (47)$$

where $\chi_s(\mathbf{r})$ is the autocovariance function associated with the interface indicator function [cf. (34)], $r = |\mathbf{r}|$, and we have invoked statistical homogeneity. The alternative Fourier representation of the surface-area variance that is dual to the direct-space representation (47) is trivially obtained by applying Parseval's theorem to (47), provided that the spectral density $\tilde{\chi}_s(\mathbf{k})$ exists:

$$\sigma_s^2(R) = \frac{1}{s^2 v_1(R)(2\pi)^d} \int_{\mathbb{R}^d} \tilde{\chi}_s(\mathbf{k}) \tilde{\alpha}(k; R) d\mathbf{k}. \quad (48)$$

A two-phase system is hyperuniform with respect to surface-area fluctuations if the spectral density $\tilde{\chi}_s(\mathbf{k})$ obeys the condition

$$\lim_{|\mathbf{k}| \to 0} \tilde{\chi}_s(\mathbf{k}) = 0, \quad (49)$$

which implies the sum rule

$$\int_{\mathbb{R}^d} \chi_s(\mathbf{r}) d\mathbf{r} = 0. \quad (50)$$

This hyperuniformity property is equivalent to requiring that the surface-area variance $\sigma_S^2(R)$ for large R goes to zero more rapidly than R^{-d}, which is the same condition as that for the volume-fraction variance discussed in the Introduction. Using precisely the same analysis as for point configurations [16,18,19], it is simple to show that three different hyperuniform scaling regimes arise from (48) when the surface-area spectral density goes to zero with the power-law form $\tilde{\chi}_s(\mathbf{k}) \sim |\mathbf{k}|^\alpha$:

$$\sigma_s^2(R) \sim \begin{cases} R^{-(d+1)}, & \alpha > 1, \\ R^{-(d+1)} \ln R, & \alpha = 1, \quad (R \to \infty). \\ R^{-(d+\alpha)}, & 0 < \alpha < 1, \end{cases} \quad (51)$$

Note that these scaling forms are exactly the same as those for volume-fraction fluctuations [cf. (5)].

B. Sphere packings

Here we make some remarks about hyperuniformity associated with specific-surface fluctuations in the case of sphere packings. To do so, we first must collect some known results for their interfacial two-point statistics. In the special instance of packings of congruent spheres of radius a in $\mathbb{R}^d$ at number density ρ, the autocovariance function $\chi_s(\mathbf{r})$ is known exactly in terms of the pair correlation function [68,101],

$$\chi_s(\mathbf{r}) = \rho\, m_s(r; a) \otimes m_s(r; a)$$
$$+ \rho^2 m_s(r; a) \otimes m_s(r; a) \otimes h(\mathbf{r}), \quad (52)$$

where

$$m_s(r; a) = \frac{\partial m_v(r; a)}{\partial a} = \delta(r - a) \quad (53)$$

is an interface indicator function for a sphere, $\delta(r)$ is a radial Dirac delta function, and $m(r; a)$ is defined by (36). Note that the first term on the right side of relation (52), which has

support in the interval $[0,2a]$, generally possesses an integrable singularity at the origin [102]. Fourier transformation of (52) gives the corresponding spectral density in terms of the structure factor [68,102],

$$\tilde{\chi}_s(\mathbf{k}) = \rho\, \tilde{m}_s^2(k; a) S(\mathbf{k}), \quad (54)$$

where $\tilde{m}_s(k; a)$ is the Fourier transform of the radial Dirac δ function (53) given by

$$\tilde{m}_s(k; a) = \frac{\partial \tilde{m}_v(k; a)}{\partial a} = \left(\frac{2\pi a}{k}\right)^{d/2} k J_{d/2-1}(ka). \quad (55)$$

The global specific surface s, defined generally by (32), is given by

$$s = \rho \tilde{m}_s(k = 0; a) = \rho s_1(a) = \frac{d\phi}{a}, \quad (56)$$

where

$$s_1(a) \equiv \frac{\partial v_1(a)}{\partial a} = \frac{d\pi^{d/2} a^{d-1}}{\Gamma(1 + d/2)} \quad (57)$$

is the surface area of a d-dimensional sphere of radius a. Thus, since $\tilde{m}_s(k; a)$ is a positive well-behaved function in the vicinity of $k = 0$, it immediately follows from expression (54) that if the underlying point process is hyperuniform and/or stealthy, then the spectral density $\tilde{\chi}_s(\mathbf{k})$ inherits the same hyperuniformity property (49). More generally, relation (54) requires that the spectral density $\tilde{\chi}_s(\mathbf{k})$ is zero at those wave vectors where $S(\mathbf{k})$ is zero (or stealthy) and at the zeros of the function $\tilde{m}_s(k; a)$.

To compare volume-fraction and surface-area fluctuation statistics to one another, we consider an example where these quantities can be calculated exactly for a sphere-packing model as density increases up to a hyperuniform state. Specifically, we consider d-dimensional sphere packings corresponding to a certain g_2-invariant process introduced by Torquato and Stillinger [16]. A g_2-invariant process is one in which a chosen non-negative form for the pair correlation function g_2 remains invariant over a nonvanishing density [103]. The upper limiting "terminal" density is the point above which the non-negativity condition on the structure factor [cf. (20)] would be violated. Thus, whenever the structure factor attains its minimum value of zero at $\mathbf{k} = 0$ at the terminal or critical density, the system, if realizable, is hyperuniform. In Ref. [16], a variety of hyperuniform g_2-invariant processes in which the number variance $\sigma_N^2(R)$ grows like the window surface area (i.e., R^{d-1}) were exactly studied in arbitrary space dimensions.

For our purposes, we use the "step-function" g_2-invariant process, namely, a $g_2(r)$ that is defined by the unit step function $\Theta(r - D)$, where $D = 2a$ is the sphere diameter. It is noteworthy that large particle configurations in one, two, and three dimensions that achieve the step function $g_2(r)$ for densities up to the terminal density ρ_c have been numerically constructed [104,105]. Interestingly, the "ghost" random-sequential-addition packing is an exactly solvable model with an identical terminal density $\rho_c = [2^d v_1(D/2)]^{-1}$ and a pair correlation function that is very nearly equal to a step function and indeed exactly approaches the step function in the large-d limit [106]. The structure factor for the step-function g_2-invariant process in the density range $0 \leqslant \rho \leqslant \rho_c$ is exactly

given by

$$S(\mathbf{k}) = 1 - \Gamma(1 + d/2)\left(\frac{2}{kD}\right)^{d/2}\left(\frac{\rho}{\rho_c}\right)J_{d/2}(kD), \quad (58)$$

where $\rho_c = [2^d v_1(D/2)]^{-1}$ is the terminal density at which the packing is hyperuniform [16] with a small-k asymptotic scaling given by

$$S(\mathbf{k}) = \frac{1}{2(d+2)}(kD)^2 + \mathcal{O}((kD))^4. \quad (59)$$

For $\rho < \rho_c$, the packing is not hyperuniform. Substitution of (58) into relations (38) and (54) yields for this model in d dimensions the associated spectral densities for the phase volumes and interface, respectively,

$$\tilde{\chi}_V(\mathbf{k}) = \rho\left(\frac{\pi D}{k}\right)^d J_{d/2}^2(kD/2)$$
$$\times \left[1 - \Gamma(1+d/2)\left(\frac{2}{kD}\right)^{d/2}\left(\frac{\rho}{\rho_c}\right)J_{d/2}(kD)\right]$$
$$(60)$$

and

$$\tilde{\chi}_S(\mathbf{k}) = \rho\left(\frac{\pi D}{k}\right)^d k^2 J_{d/2-1}^2(kD/2)$$
$$\times \left[1 - \Gamma(1+d/2)\left(\frac{2}{kD}\right)^{d/2}\left(\frac{\rho}{\rho_c}\right)J_{d/2}(kD)\right].$$
$$(61)$$

(Note that formula (60) was reported and studied elsewhere [91].) At the terminal density ρ_c, these spectral functions also go to zero quadratically in k in the limit $k \to 0$ such that

$$\tilde{\chi}_V(\mathbf{k}) = \frac{1}{2(d+2)4^d v_1(1)}(kD)^2 + \mathcal{O}((kD))^4 \quad (62)$$

and

$$\tilde{\chi}_S(\mathbf{k}) = \frac{d^2}{2(d+2)4^{d-1}v_1(1)}(kD)^2 + \mathcal{O}((kD))^4, \quad (63)$$

but the latter has a coefficient that grows quadratically faster in the dimension relative to that in the former.

Figure 3 shows the two spectral functions, $\tilde{\chi}_V(\mathbf{k})$ and $\tilde{\chi}_S(\mathbf{k})$, for the step function g_2-invariant packing process in three dimensions at the terminal density $\rho_c = 3/(4\pi)$, as obtained from (38), (54), and (58) with $a = D/2$. Figure 4 depicts the associated local variances for the same system, as obtained from these spectral functions and relations (29) and (48). Notice that the surface-area spectral function exhibits stronger and longer-ranged correlations compared to the volume-fraction spectral function, indicating that the former is a more sensitive microstructural descriptor. Figure 4 depicts the corresponding local variances for the same system. Similarly, while the corresponding local variances decay like R^{-4} for large R, the surface-area variance does so at a slower rate relative to the volume-fraction counterpart.

The aforementioned results for the surface-area pair statistics were generalized to the case of sphere packings with a continuous or discrete size distribution [68,97]. These
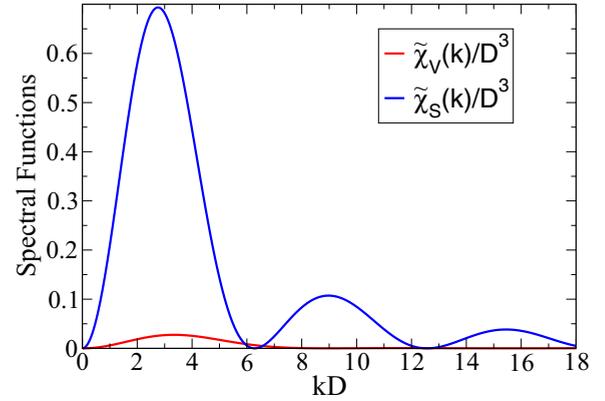

FIG. 3. Comparison of the two hyperuniform spectral functions $\tilde{\chi}_V(k)$ (lower curve) and $\tilde{\chi}_S(k)$ versus wave number k for a sphere packing corresponding to the step-function g_2-invariant process in three dimensions at the hyperuniform terminal density $\rho_c = 3/(4\pi)$ [16]. Here D is the diameter of a hard sphere.

results are collected in the Appendix in order to describe the conditions under which they are "multihyperuniform."

V. RANDOM SCALAR FIELDS AND HYPERUNIFORMITY

Here we generalize the hyperuniformity concept to random scalar fields in $\mathbb{R}^d$. Such fields can arise in a variety of physical contexts, including concentration and temperature fields in heterogeneous and porous media [68,107] as well as in turbulent flows [108,109], laser speckle patterns [110–113], and temperature fluctuations associated with the cosmic microwave background [5,114]. Other examples include spatial patterns that arise in biological and chemical systems that have been theoretically described by, for example, Cahn-Hilliard [99] and Swift-Hohenberg equations [100]. In what follows, we derive the relevant equations to quantify hyperuniform scalar fields, present illustrative calculations, and remark on two-phase media that result from level cuts.
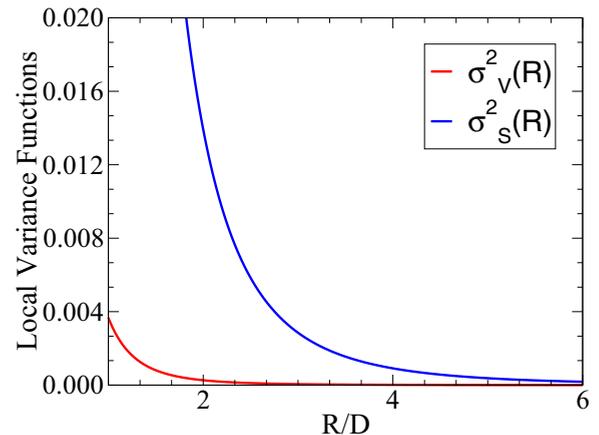

FIG. 4. Comparison of the volume-fraction variance $\sigma_V^2(R)$ (lower curve) and surface-area variance $\sigma_S^2(R)$ versus window sphere radius R for a sphere packing corresponding to the step-function g_2-invariant process in three dimensions at the hyperuniform terminal density $\rho = 3/(4\pi)$ [16]. Here D is the diameter of a hard sphere.

A. Local field fluctuations

Consider a statistically homogeneous random scalar field $F(\mathbf{x})$ in $\mathbb{R}^d$ that is real valued with an autocovariance function

$$\psi(\mathbf{r}) = \langle [F(\mathbf{x}_1) - \langle F(\mathbf{x})_1 \rangle][F(\mathbf{x}_2) - \langle F(\mathbf{x}_2) \rangle]\rangle, \quad (64)$$

where we have invoked the statistical homogeneity of the field, since $\mathbf{r} = \mathbf{x}_2 - \mathbf{x}_1$, which is a d-dimensional vector. We assume that the associated spectral density $\tilde{\psi}(\mathbf{k})$ (Fourier transform of the autocovariance) exists. The hyperuniformity condition is simply that the non-negative spectral density obeys the small-wave-number condition

$$\lim_{|\mathbf{k}| \to \mathbf{0}} \tilde{\psi}(\mathbf{k}) = 0, \quad (65)$$

which implies the sum rule

$$\int_{\mathbb{R}^d} \psi(\mathbf{r}) d\mathbf{r} = 0. \quad (66)$$

The local variance associated with fluctuations in the field, denoted by $\sigma_F^2(R)$, is related to the autocovariance function or spectral function in the usual way:

$$\sigma_F^2(R) = \frac{1}{v_1(R)} \int_{\mathbb{R}^d} \psi(\mathbf{r}) \alpha(r; R) d\mathbf{r},$$
$$= \frac{1}{v_1(R)(2\pi)^d} \int_{\mathbb{R}^d} \tilde{\psi}(\mathbf{k}) \tilde{\alpha}(k; R) d\mathbf{k}. \quad (67)$$

While the main focus of this section is continuous random scalar fields, it should be noted that when simulating random fields on the computer or when extracting them from experimentally obtained images, one must inevitably treat discrete or digitized renditions of the fields. The "pixels" or "voxels" (smallest components of the digitized systems in 2D and 3D dimensions, respectively) take on grayscale intensities that span the intensity range associated with the continuous field. Thus, the discrete versions of relations (64) and (67) are to be applied in such instances; see, for example, Ref. [115].

B. Random fields derived from point configurations

Now we prove that a class of fields derived from underlying hyperuniform point configurations are themselves hyperuniform. Consider a general ensemble of point configurations of N points in a large region of volume V in $\mathbb{R}^d$. Let $K(\mathbf{x}; \mathbf{C})$ represent a non-negative dimensionless scalar kernel function that is radial in $\mathbf{x}$ and sufficiently localized so that its Fourier transform exists. Here $\mathbf{C}$ represents a set of parameters that characterizes the shape of the radial function. Following Blumenfeld and Torquato [115], the random scalar field $F(\mathbf{x})$ is defined as a convolution of the microscopic density and the kernel, i.e.,

$$F(\mathbf{x}) = \int_{\mathbb{R}^d} n(\mathbf{x}') K(\mathbf{x} - \mathbf{x}') d\mathbf{x}' = \sum_{i=1}^{N} K(\mathbf{x} - \mathbf{r}_i), \quad (68)$$

where we have stopped indicating the explicit dependence of the kernel on the parameter set $\mathbf{C}$. It is seen that the effect of the kernel is to smooth out the point "intensities." Ensemble averaging (68) and using the definition (7) yields

the expectation of the field,

$$\langle F(\mathbf{x}) \rangle = \left\langle \sum_{i=1}^{N} K(\mathbf{x} - \mathbf{r}_i) \right\rangle$$
$$= \int_V \int_V \cdots \int_V \sum_{i=1}^{N} K(\mathbf{x} - \mathbf{r}_i) P_N(\mathbf{r}^N) d\mathbf{r}^N$$
$$= \int_V \rho_1(\mathbf{r}_1) K(\mathbf{x} - \mathbf{r}_1) d\mathbf{r}_1$$
$$= \rho \int_{\mathbb{R}^d} K(\mathbf{x}) d\mathbf{x}, \quad (69)$$

where in the last line we have invoked the statistical homogeneity of the field and hence have taken the thermodynamic limit. Similarly, the autocorrelation function associated with the field is given by

$$\langle F(\mathbf{x}) F(\mathbf{x} + \mathbf{r}) \rangle = \left\langle \sum_{i=1}^{N} K(\mathbf{x} - \mathbf{r}_i) K(\mathbf{x} + \mathbf{r} - \mathbf{r}_i) \right\rangle$$
$$+ \left\langle \sum_{i \neq j}^{N} K(\mathbf{x} - \mathbf{r}_i) K(\mathbf{x} + \mathbf{r} - \mathbf{r}_j) \right\rangle$$
$$= \rho K(\mathbf{r}) \otimes K(\mathbf{r})$$
$$+ \rho^2 K(\mathbf{r}) \otimes K(\mathbf{r}) \otimes h(\mathbf{r}) + \langle F \rangle^2, \quad (70)$$

where $h(\mathbf{r})$ is the total correlation function for the point configuration defined by (13). Thus, the autocovariance function $\psi(\mathbf{r})$, defined generally by (64), is given by

$$\psi(\mathbf{r}) = \rho K(\mathbf{r}) \otimes K(\mathbf{r}) + \rho^2 K(\mathbf{r}) \otimes K(\mathbf{r}) \otimes h(\mathbf{r}). \quad (71)$$

Fourier transforming (71) yields the corresponding nonnegative spectral density

$$\tilde{\psi}(\mathbf{k}) = \rho \tilde{K}^2(\mathbf{k}) S(\mathbf{k}), \quad (72)$$

where $\tilde{K}(\mathbf{k})$ is the Fourier transform of the kernel $K(\mathbf{x})$ and $S(\mathbf{k})$ is the ensemble-averaged structure factor [cf. (20)]. We see from (72) that if the underlying point process is hyperuniform, i.e., $S(\mathbf{k})$ tends to zero in the limit $|\mathbf{k}| \to 0$ and $\tilde{K}(\mathbf{k})$ is well-behaved at $\mathbf{k} = \mathbf{0}$, the spectral density obeys the hyperuniformity condition (65).

As a simple example, consider the Gaussian kernel function

$$K(\mathbf{r}) = \exp[-(r/a)^2], \quad (73)$$

where a is a characteristic length scale that is proportional to the standard deviation of the Gaussian. The corresponding Fourier transform is given by

$$\tilde{K}(\mathbf{k}) = \pi^{d/2} a^d \exp[-(ka)^2/4]. \quad (74)$$

Consider the hyperuniform structure factor (58) for the step-function g_2-invariant packing. Substitution of (58) into relation (38) yields the associated spectral density for this model in d dimensions:

$$\tilde{\psi}(\mathbf{k}) = \rho \pi^{d/2} a^d \exp[-(ka)^2/4]$$
$$\times \left[1 - \Gamma(1 + d/2) \left(\frac{2}{kD} \right)^{d/2} \left(\frac{\rho}{\rho_c} \right) J_{d/2}(kD) \right]. \quad (75)$$
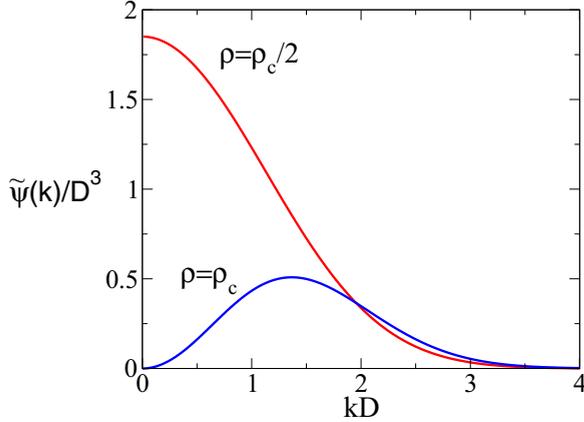
FIG. 5. The spectral function $\tilde{\psi}(\mathbf{k})$ versus wave number k for the three-dimensional Gaussian field derived from the step-function g_2-invariant packing for a nonhyperuniform case ($\rho = \rho_c/2$) and the unique hyperuniform instance ($\rho = \rho_c$). Here $\rho_c = 3/(4\pi)$ and $a = D$, where D is a hard-sphere diameter.

Substituting this expression into (72) with $\rho = \rho_c$ and expanding the spectral density in powers of k^2 about the origin yields

$$\tilde{\psi}(\mathbf{k}) = \frac{\pi^{d/2}\rho_c a^d}{2(d+2)}k^2 + \mathcal{O}(k^4). \qquad (76)$$

Note that this scalar field is hyperuniform such that $\tilde{\psi}(\mathbf{k})$ goes to zero quadratically in k as the wave number tends to zero, independent of the space dimension d.

Figure 5 shows this spectral function $\tilde{\psi}(\mathbf{k})$ in the special case of three dimensions at the hyperuniform terminal density as well as at a nonhyperuniform case. The scaled corresponding variances, obtained from relations (67) and (75), are shown in Fig. 6. Note that since $\sigma_F^2(R)$ for the nonhyperuniform case must decay like R^{-3} for large R, the
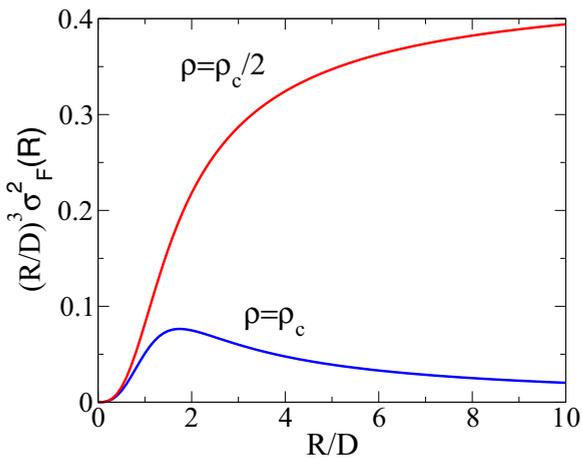

FIG. 6. Comparison of the field variance $\sigma_F^2(R)$ [multiplied by $(R/D)^3$] versus window sphere radius R/D for the three-dimensional Gaussian field derived from the step-function g_2-invariant packing for a nonhyperuniform case ($\rho = \rho_c/2$) and the hyperuniform case ($\rho = \rho_c$). Here $\rho_c = 3/(4\pi)$ and $a = D$, where D is a hard-sphere diameter.

product $R^3\sigma_V^2(R)$ asymptotes to a constant value. By contrast, the product $R^3\sigma_F^2(R)$ for $\rho = \rho_c$ decays like R^{-1} for large R, as it should for this three-dimensional hyperuniform random scalar field.

C. Level cuts of random fields

In the random-field approach to modeling the microstructure of random media, the interface between the phases is defined by level cuts of random fields [115–120]. There is great flexibility in the choice of the random field $F(\mathbf{x})$ and hence in the class of microstructures that can be produced. This approach is particularly useful in modeling *bicontinuous* media (two-phase media in which each phase percolates), such as microemulsions [116], carbonate rocks [119], Vycor glass [119], amorphous alloys [120], and aerogels [121]. It is noteworthy that the use of level cuts of random fields to create disordered hyperuniform two-phase or multiphase heterogeneous systems has heretofore not been carried out and thus represents a fruitful area for future research. To derive a hyperuniform two-phase medium from a thresholded random field $F(\mathbf{r})$, the field must possess the special correlations required to yield an autocovariance function $\chi_V(\mathbf{r})$ that satisfies the sum rule (30).

VI. DIVERGENCE-FREE RANDOM VECTOR FIELDS AND HYPERUNIFORMITY

It is natural to generalize the hyperuniformity concept for scalar fields to random vector fields. In order to narrow the enormous possibilities in this substantially broader context, we focus primarily on divergence-free random vector fields, but the basic ideas apply to more general vector fields. Excellent physical examples within this class of fields occur in heterogeneous media, including divergence-free heat, current or mass flux fields, divergence-free electric displacement fields associated with dielectrics, divergence-free magnetic induction fields, and divergence-free low-Reynolds-number velocity fields [68,107]. Incompressible turbulent-flow fields provide yet other very well-known set of examples [108,109]. Here we derive the relevant equations to quantify hyperuniform vector fields, present illustrative calculations, and make contact with turbulent-flow spectra.

Consider a statistically homogeneous divergence-free (solenoidal) random vector field $\mathbf{u}(\mathbf{x})$ in $\mathbb{R}^d$ that is real valued with zero mean, i.e.,

$$\nabla \cdot \mathbf{u}(\mathbf{x}) = 0, \qquad (77)$$

where

$$\langle \mathbf{u}(\mathbf{x}) \rangle = 0. \qquad (78)$$

Taking the Fourier transform of (77) yields

$$\mathbf{k} \cdot \tilde{\mathbf{u}}(\mathbf{k}) = 0 \quad \text{for all } \mathbf{k}, \qquad (79)$$

where $\tilde{\mathbf{u}}(\mathbf{k})$ is the Fourier transform of $\mathbf{u}(\mathbf{x})$. A key quantity is the autocovariance function $\Psi_{ij}(\mathbf{r})$ ($i,j = 1,2,\ldots,d$) associated with the vector field $\mathbf{u}(\mathbf{x})$, which is a second-rank tensor field defined by

$$\Psi_{ij}(\mathbf{r}) = \langle u_i(\mathbf{x})u_j(\mathbf{x} + \mathbf{r}) \rangle, \qquad (80)$$

where we have invoked the statistical homogeneity of the field. The divergence-free condition (77) implies

$$\frac{\partial \Psi_{ij}(\mathbf{r})}{\partial r_i} = 0 \tag{81}$$

and

$$\frac{\partial \Psi_{ij}(\mathbf{r})}{\partial r_j} = 0, \tag{82}$$

where the second equation follows from the symmetry property $\Psi_{ij}(\mathbf{r}) = \Psi_{ji}(-\mathbf{r})$ and Einstein indicial summation notation is implied. Taking the Fourier transforms of (81) and (82) yield the identities

$$k_i \tilde{\Psi}_{ij}(\mathbf{k}) = k_j \tilde{\Psi}_{ij}(\mathbf{k}) = 0 \quad \text{for all } \mathbf{k}, \tag{83}$$

where $\tilde{\Psi}_{ij}(\mathbf{k})$ is the spectral density tensor, i.e., the Fourier transform of the autocovariance tensor (80). The real-valued spectral density tensor is positive semidefinite; i.e., for an arbitrary real vector $\mathbf{a}$,

$$a_i \tilde{\Psi}_{ij}(\mathbf{k}) a_j \geqslant 0 \quad \text{for all } \mathbf{k}. \tag{84}$$

From the theory of turbulence of an incompressible fluid [108,109], it is well known that if an arbitrary divergence-free vector field $\mathbf{u}(\mathbf{x})$ is also isotropic, then the spectral density tensor must take the general form

$$\tilde{\Psi}_{ij}(\mathbf{k}) = \left(\delta_{ij} - \frac{k_i k_j}{k^2} \right) \tilde{\psi}(k), \tag{85}$$

where δ_{ij} is the Kronecker δ or identity tensor and $\tilde{\psi}(k)$ is a non-negative scalar radial function of the wave number $k = |\mathbf{k}|$. A random vector field is isotropic if all of its associated n-point correlation functions are independent of translations, rotations, and reflections of the coordinates. Note that the trace of $\tilde{\Psi}_{ij}(\mathbf{k})$ is trivially related to $\tilde{\psi}(k)$, i.e.,

$$\tilde{\Psi}_{ii}(\mathbf{k}) = (d-1) \tilde{\psi}(k), \tag{86}$$

and so we see that

$$\tilde{\Psi}_{ii}(\mathbf{k} = \mathbf{0}) = (d-1) \tilde{\psi}(k=0) = \int_{\mathbb{R}^d} \Psi_{ii}(\mathbf{r}) d\mathbf{r} \tag{87}$$

and

$$\Psi_{ii}(\mathbf{r} = \mathbf{0}) = \frac{(d-1)}{(2\pi)^d} \int_{\mathbb{R}^d} \tilde{\psi}(k) d\mathbf{k}. \tag{88}$$

Now if the radial function $\tilde{\psi}(k)$ is continuous but positive at $k = 0$ (not hyperuniform), it immediately follows from the form (85) that the spectral tensor can only be hyperuniform in *certain directions*. For example, the component $\tilde{\Psi}_{11}(\mathbf{k})$ is zero for $k = k_1$ (all wave vectors along the k_1 axis) and the component $\tilde{\Psi}_{12}(\mathbf{k})$ is zero whenever $k_1 = 0$ or $k_2 = 0$. The fact that the value of $\tilde{\Psi}_{11}(\mathbf{k})$ depends on the direction in which the origin is approached means that it is nonanalytic at $\mathbf{k} = \mathbf{0}$. On the other hand, if $\tilde{\psi}(k)$ is hyperuniform and continuous at $k = 0$, then each component of $\tilde{\Psi}_{ij}(\mathbf{k})$ will inherit the radial hyperuniformity of $\tilde{\psi}(k)$, and hence is independent of the direction in which the origin is approached. For example, consider the situation in which $\tilde{\psi}(k)$ admits the small-wave-number expansion

$$\tilde{\psi}(k) = a_1 |\mathbf{k}|^\alpha + o(|\mathbf{k}|^\alpha), \tag{89}$$

where α is a positive constant and o signifies higher-order terms. Note that whenever α is a noninteger or odd integer, $\tilde{\psi}(k)$ is a nonanalytic function at the origin due to a derivative discontinuity. (An analytic radial function would admit an expansion in even powers of the wave number only.) For any $\alpha > 0$, substitution of (89) in (85) reveals that the spectral tensor is radially hyperuniform near $\mathbf{k} = \mathbf{0}$ such that it vanishes as $|\mathbf{k}|^\alpha$.

We conclude that we need an even more general hyperuniformity concept in the case of a spectral tensor, namely, one in which hyperuniformity depends on the direction in which the origin is approached in Fourier space. Let $\mathbf{k}_Q$ represent a d-dimensional unit vector emanating from the origin $\mathbf{k} = \mathbf{0}$. We say that the field is hyperuniform for a particular component $i = I$ and $j = J$ of the spectral tensor of a vector field (isotropic or not) in the direction $\mathbf{k}_Q$ if

$$\lim_{t \to 0} \tilde{\Psi}_{IJ}(t\mathbf{k}_Q) = \mathbf{0}, \tag{90}$$

where t is a scalar parameter. Note that there are many different unit vectors (directions) for a particular spectral tensor that can satisfy this condition, whether this set is countable or it is uncountable because these unit vectors can occur in a continuous range of directions. Moreover, if the condition applies independent of the direction of the unit vector, then it reduces to the standard spectral definition of hyperuniformity.

To illustrate the hyperuniformity concept in the context of a divergence-free isotropic vector field, let us consider the hyperuniform radial function

$$\tilde{\psi}(k) = c(d)(ka) \exp[-(ka)^2], \tag{91}$$

where

$$c(d) = \frac{\Gamma(d/2) a^d}{2^d \pi^{d/2} \Gamma[(d+1)/2]}. \tag{92}$$

This is a valid (non-negative) spectral function in any dimension with an associated autocovariance function $\psi(r)$ such that $\psi(r = 0) = 1$. For visual purposes, we examine the two-dimensional outcome when (91) is substituted into the spectral tensor (85). Figure 7 shows three components of this symmetric tensor and the radial function $\tilde{\psi}(k)$. The hyperuniformity property in a compact region around the origin for all components is readily visible.

It is instructive to place some well-known results from the theory of isotropic turbulence in the context of the generalization of hyperuniformity to divergence-free random vector fields. For three-dimensional incompressible turbulent flow with an isotropic velocity field, the radial function $\tilde{\psi}(k)$ appearing in (85) is simply related to the so-called *energy spectrum* of the velocity field, $E(k)$, via the expression $\tilde{\psi}(k) = E(k)/(4\pi k^2)$. Thus, we see from the analysis given above that if $E(k)$ goes to zero faster than k^2 in the limit $k \to 0$, then each component of the spectral tensor $\tilde{\Psi}_{ij}(\mathbf{k})$ will inherit the radial hyperuniformity of $\tilde{\psi}(k)$, and hence is independent of the direction in which the origin is approached. An example of such energy spectra is one due to Batchelor [108], where $E(k) \sim k^4$ or $\tilde{\psi}(k) \sim k^2$ in the small wave-number limit. Note that the corresponding radial autocovariance function $\psi(r)$ decays to zero for large r exponentially fast. On the other hand, if the energy spectrum goes to zero like k^2 or slower in
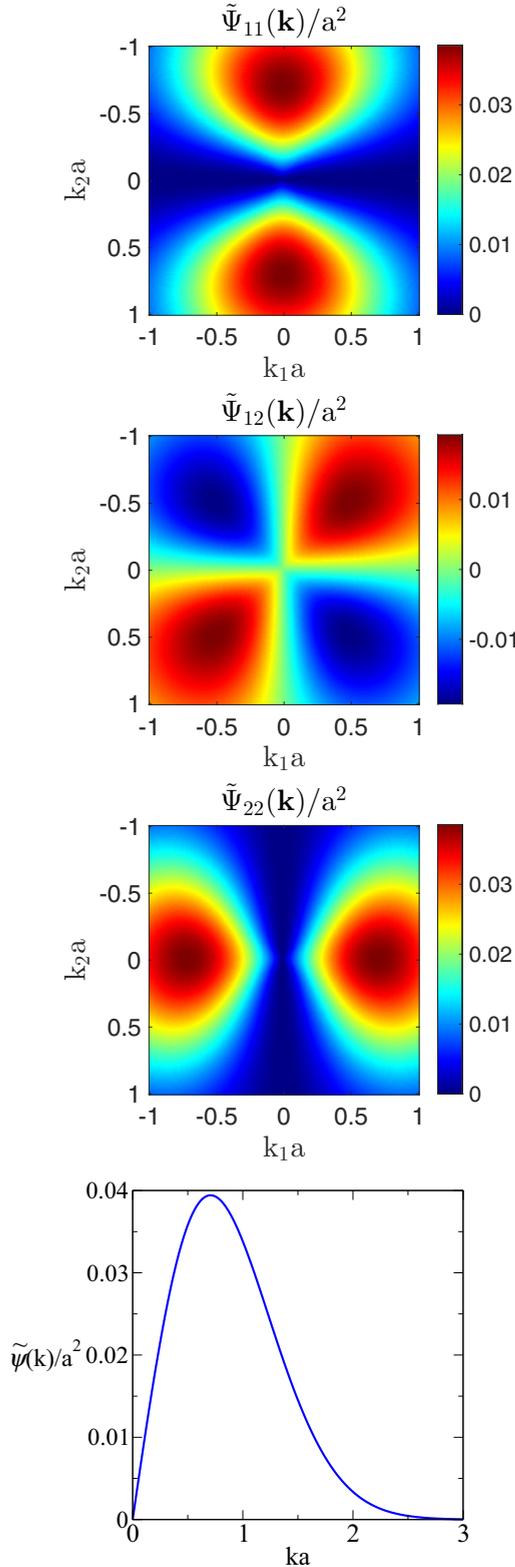
FIG. 7. Spectral patterns for the tensor components of a divergence-free isotropic vector field in $\mathbb{R}^2$ generated from the radial function (91) with $d = 2$, depicted in the bottom panel. Note that unlike the non-negative 11 and 22 components, the 12 component can be both positive and negative, and so its color map indicating zero intensity (darkest shade) is different from those for the diagonal components.
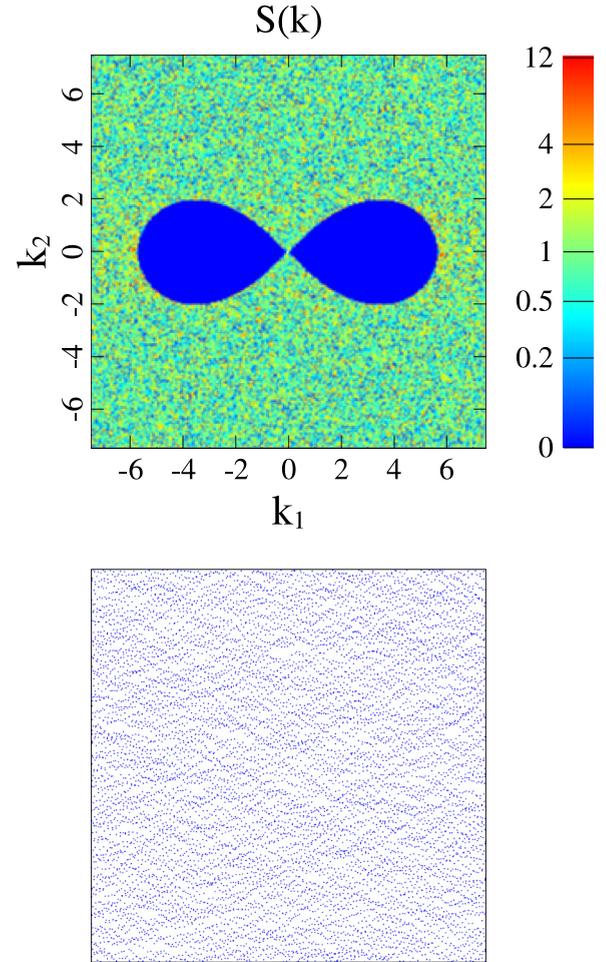

FIG. 8. (Top) A targeted scattering pattern showing a lemniscate region around the origin in which the scattering intensity is exactly zero (darkest shade). This "stealthy" pattern clearly shows that hyperuniformity depends on the direction in which the origin $\mathbf{k} = \mathbf{0}$ is approached. (Bottom) A statistically anisotropic ground-state configuration of 10 000 particles that corresponds to the unusual scattering pattern shown in the top panel, which is generated using the collective-coordinate optimization procedure [21,25,26] in a square simulation box under periodic boundary conditions.

the limit $k \to 0$, then the value of the spectral tensor will be hyperuniform only in special directions. An example within the class of energy spectra is one due to Saffman [122], where $E(k) \sim k^2$ or $\tilde{\psi}(k) \sim$ constant in the small wave-number limit. Here $\tilde{\Psi}_{ij}(\mathbf{k})$ is nonanalytic at $\mathbf{k} = \mathbf{0}$. Of course, the significance of energy spectra in turbulence *vis a vis* hyperuniformity was previously not discussed.

VII. STRUCTURAL ANISOTROPY AND HYPERUNIFORMITY

Other classes of disordered systems in which "directional" hyperuniformity is relevant include many-particle and heterogeneous systems that are statistically anisotropic, but otherwise statistically homogeneous; see Figs. 8 and 9 for two illustrations. In such cases, the spectral function conditions (1), (4), and (49) should be replaced with the following ones,
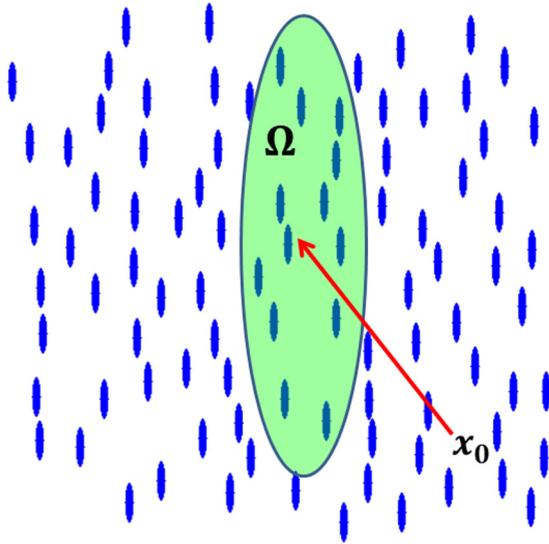
FIG. 9. Schematic illustration of a statistically homogeneous and anisotropic nematic liquid crystal configuration. An appropriately shaped window that occupies region Ω is also shown. Here $\mathbf{x_0}$ denotes both the centroidal position and orientation of the window, the latter of which is chosen generally from a prescribed probability distribution that depends on the specific structure of interest.
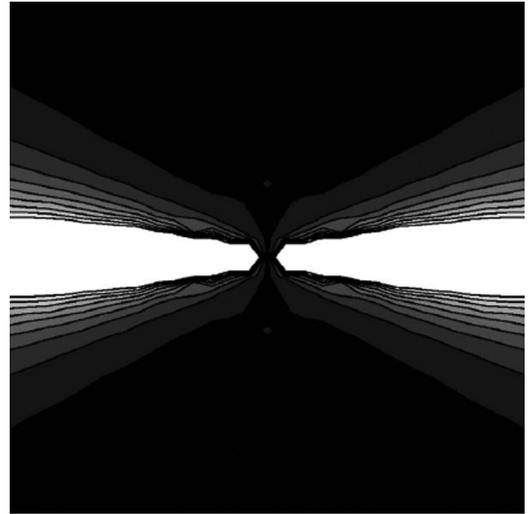

FIG. 10. Anisotropic structure factor of a colloidal ferrofluid in the plane in which the particle chains align, as obtained from Fig. 6 of Ref. [126]. Dark and light regions indicate low and high intensities, respectively. Note that depending on the direction in which the origin is approached, the structure factor can exhibit effective hyperuniformity.

respectively,

$$\lim_{t \to 0} S(t\mathbf{k}_Q) = 0, \tag{93}$$

$$\lim_{t \to 0} \tilde{\chi}_V(t\mathbf{k}_Q) = 0, \tag{94}$$

$$\lim_{t \to 0} \tilde{\chi}_s(t\mathbf{k}_Q) = 0, \tag{95}$$

where the vector $\mathbf{k}_Q$ is defined in Sec. VI.

Are structurally anisotropic configurations associated with such exotic spectral functions realizable? To vividly demonstrate that the answer to this question is in the affirmative, the collective-coordinate optimization scheme [21,25,26,123] is employed to produce a many-particle system that is hyperuniform in only certain directions in Fourier space. This powerful procedure by construction enables the structure factor to be constrained to take exact targeted values at a subset of wave vectors. Whenever the structure factor is constrained to be exactly zero for this subset of wave vectors, the resulting configuration exactly corresponds to the classical ground state of a long-ranged but bounded pair interaction [124]. For example, one can target stealthy and hyperuniform structure factors that vanish in a spherical region around the origin (as in Fig. 1) such that the associated disordered particle configurations are statistically homogeneous and isotropic ground states [21,25,26]. Targeted anisotropic structure factors have been attained that correspond to statistically anisotropic ground-state structures with directional pair interactions [123], but none of the specific targets computed there were hyperuniform. Here we target a lemniscate region around the origin $\mathbf{k} = \mathbf{0}$ in Fourier space in which scattering is completely suppressed; i.e., this entire region is stealthy, but hyperuniform in only certain directions (see the top panel of Fig. 8). The corresponding disordered ground states are due

to directional long-ranged pair interactions that are stronger in the horizontal direction than in the vertical direction, and hence are characterized by like-linear "filamentary" chains of particles that run more or less horizontally. Such an example is shown in the bottom panel of Fig. 8.

These ground states are characterized by directional-dependent physical properties, including optical, acoustic, and elastic behaviors. Interestingly, although such anisotropic ground-state configurations cannot support shear (for similar reasons as in their isotropic counterparts [26]), they are generally elastically anisotropic because the stress tensor is asymmetric, as will be detailed in a future study. In particular, the asymmetry of the stress tensor is associated with internal force couples that resist out-of-plane torques. While such behavior is known to occur in liquid crystals and predicted by continuum elastic theories [125], our results are distinguished because the asymmetry of the stress tensor arises from a microscopic statistical-mechanical model of interacting *structureless (point)* particles. To our knowledge, such a microscopic model has heretofore not been identified.

Many-particle systems that respond to external fields are often characterized by anisotropic structure factors and hence provide a class of systems where directional hyperuniformity can potentially arise. Huang, Wang, and Holm [126] have carried out molecular dynamics simulations of colloidal ferrofluids subjected to external fields that capture the salient structural features observed in corresponding experimental systems as measured by the structure factor. Structural anisotropy arises in these systems due to the formation of particle chains that tend to align in the direction of the applied magnetic field. Figure 10 shows an anisotropic structure factor taken from Ref. [126]. It is apparent that, depending on the direction in which the origin is approached, the structure factor can exhibit effective hyperuniformity.

We can generalize the expressions for the number variance for point configurations and variances for a structurally anisotropic two-phase medium by replacing spherical windows with an appropriately shaped nonspherical window occupying region Ω with an orientation distribution that maximizes sensitivity to direction. This general formulation was given in Ref. [16] for point configurations, but no explicit calculations were presented. Figure 9 schematically depicts a statistically homogeneous, anisotropic nematic liquid crystal configuration of particles, and an appropriate window shape and orientational distribution to distinguish "directional" fluctuations associated with either the centroidal positions, volume fraction, or interfacial area of the particles. It is clear that window sampling in the direction indicated in Fig. 9 will produce fluctuations that are different from those obtained by sampling in the orthogonal direction.

Note that the volume-fraction formulas for the autocovariance $\chi_V(\mathbf{r})$ and spectral density $\tilde{\chi}_V(\mathbf{k})$ for sphere packings presented in Sec. III apply as well to the more general class of packings of oriented nonspherical particles by a simple replacement of the spherical particle indicator function (36) with the following one for a nonspherical particle that occupies a region ω,

$$m_v(\mathbf{r};\mathbf{a}) = \begin{cases} 1, & \mathbf{r} \in \omega, \\ 0, & \mathbf{r} \notin \omega, \end{cases} \tag{96}$$

where the vector $\mathbf{r}$ emanates from the particle centroid and the vector $\mathbf{a}$ represents the set of parameters that defines the shape of the particle. For example, for a d-dimensional ellipsoid, this is given explicitly by

$$m_v(\mathbf{r};\mathbf{a}) = \begin{cases} 1, & \frac{r_1^2}{a_1^2} + \frac{r_2^2}{a_2^2} + \cdots + \frac{r_d^2}{a_d^2} \leqslant 1, \\ 0, & \text{otherwise}, \end{cases} \tag{97}$$

where r_i $(i = 1, 2, \ldots, d)$ is the ith the Cartesian component of $\mathbf{r}$ and $a_1, a_2, \ldots, a_d$ are the semiaxes of the ellipsoid. Of course, the structural anisotropy for configurations of oriented particles of general shape is reflected in a total correlation function $h(\mathbf{r})$ or an autocovariance $\chi_V(\mathbf{r})$ that depends not only on the magnitude but direction of $\mathbf{r}$. Observe also that the calculation of $h(\mathbf{r})$ and $\chi_V(\mathbf{r})$ for the special case of oriented ellipsoids is greatly simplified by exploiting the fact that an ellipsoid is an affine scale transformation of a sphere [127,128].

Similarly, the surface-area formulas for the autocovariance $\chi_S(\mathbf{r})$ and spectral density $\tilde{\chi}_S(\mathbf{k})$ for sphere packings presented in Sec. IV B still apply to packings of oriented nonspherical particles when the radial functions $m_s(r;a)$ are replaced with the appropriate vector-dependent interface indicator function for a particle $m_s(\mathbf{r};\mathbf{a})$, which is a generalized function that has measure only on the particle surface. As in the case of anisotropic point configurations, the variances for both volume fraction and surface area, $\sigma_V^2(R)$ and $\sigma_S^2(R)$, for sphere packings using spherical windows of radius R can be generalized to allow for anisotropic packings of nonspherical particles with an appropriately shaped nonspherical window [16].

VIII. CONCLUSIONS AND DISCUSSION

We have generalized the hyperuniformity concept in four different directions: (1) interfacial-area fluctuations in hetero-geneous materials; (2) random scalar fields; (3) divergence-free random vector fields; and (4) statistically anisotropic many-particle systems and heterogeneous media. These gen-eralizations provide theoreticians and experimentalists new research avenues to understand a very broad range of phenomena across a variety of fields through the hyperuniformity "lens."

The surface-area variance $\sigma_S^2(R)$ and associated spectral density function $\tilde{\chi}_S(\mathbf{k})$ could play a new and major role in characterizing the microstructure of two-phase systems, including fluid-saturated porous media, physical properties that intimately depend on the interface geometry, such as reaction rates and fluid permeabilities [68], and evolving microstructures that depend on interfacial energies (e.g., spinodal decomposition). It should not go unnoticed that the hyperuniformity concept for two-phase media specified by the volume-fraction and surface-area variances $\sigma_V^2(R)$ and $\sigma_S^2(R)$, respectively, are fluctuations that describe two of the Minkowski functionals [129]. In the case of sphere packings, we showed that the surface-area spectral function exhibits stronger and longer-ranged correlations compared to the volume-fraction spectral function, indicating that the former is a more sensitive microstructural descriptor.

Little is known about the hyperuniformity of random scalar fields and its potential significance. Now that we know what to look for in such contexts, exploration of this uncharted territory may prove to be profitable. For example, one could imagine designing random scalar fields to be hyperuniform (e.g., laser speckle patterns) for photonics applications [111,113].

Our generalization of the hyperuniformity concept to random vector fields is the most encompassing to date. This setting generally involves a spectral density tensor, which, of course, contains random scalar fields as special cases. Even the restricted class of divergence-free vector fields that we focused on here revealed the need to extend the "isotropic" hyperuniformity notion, since the spectral tensor is nonanalytic at zero wave vector; i.e., it depends on the direction in which the origin in Fourier space is approached. Among other results, we placed well-known energy spectra from the theory of isotropic turbulence in the context of this generalization of hyperuniformity. More generally, our work provides a motivation to design random vector fields with targeted directional hyperuniform spectra, which heretofore has never been considered.

Structurally anisotropic many-particle and heterogeneous systems can also possess directional hyperuniformity. To illustrate the implications of this generalization, we pre-sented a disordered directionally hyperuniform many-particle configuration that remarkably is the ground state associated with a bounded anisotropic pair potential; see Fig. 8. These filamentarylike ground-state configurations will be character-ized by directional-dependent physical properties, including optical and elastic behaviors. Interestingly, such anisotropic ground-state configurations generally will possess internal force couples that resist out-of-plane torques, which will be shown in detail elsewhere. Based on our previous investiga-tions using disordered isotropic ground-state configurations to produce disordered dielectric network solids with large isotropic band gaps [36,60], we expect that one can design directional hyperuniform ground-state configurations to yield disordered network solids that can be tuned to have photonic

and acoustic band gaps with widths that are relatively uniform for a continuous range of directions and no band gaps for a different continuous range of directions. Such tunability could have technological relevance for manipulating light and sound waves in ways heretofore not thought possible. Moreover, materials made of dense disordered scatterers that are directionally hyperuniform can be designed to be transparent in selected directions, as a recent study of traditional hyperuniform systems would suggest [48].

Directional structural hyperuniformity raises the interesting possibility that there may exist disordered many-particle systems in equilibrium that at positive temperature T are incompressible in certain directions and compressible in other directions, a highly unusual situation. To understand this proposition, it is useful to recall the well-known fluctuation-compressibility theorem for a single-component many-particle system in equilibrium at number density ρ and temperature T,

$$\rho k_B T \kappa_T = \lim_{|\mathbf{k}| \to 0} S(\mathbf{k}), \tag{98}$$

where κ_T is the isothermal compressibility. We see that in order to have a hyperuniform system at positive T, the isothermal compressibility must be zero; i.e., the system must be incompressible [19,20]. A well-known model that exhibits such behavior is the one-component plasma [130]. However, if the system possesses directional structural hyperuniformity, relation (98) no longer applies. Therefore, one must first generalize this fluctuation-compressibility theorem to account for directional elastic responses of the system to different components of stress due to nonanalyticities of the spectral density at the origin. While (98) has been extended to treat crystals under certain restrictions [131], to our knowledge, there is currently no known generalization of (98) that accounts for the anisotropic elastic response of a disordered equilibrium system to directional stresses due to nonanalytic spectral densities. Such a generalization of the fluctuation-compressibility theorem would enable one to quantify the directions in which the aforementioned hypothesized disordered system is incompressible or compressible. This represents an intriguing area for future research. In particular, this possibility challenges experimentalists to search for such exotic states of matter.

Finally, we note that the hyperuniformity concept has recently been generalized to spin systems, including a capability to construct disordered stealthy hyperuniform spin configurations as ground states [132]. The implications and significance of the existence of such disordered spin ground states warrant further study, including whether their bulk physical properties and excited states, like their many-particle system counterparts, are singularly remarkable and can be experimentally realized.

APPENDIX: MULTIHYPERUNIFORMITY AND SURFACE-AREA FLUCTUATIONS IN POLYDISPERSE SPHERE PACKINGS

Both the autocovariance function and the associated spectral density for packings of hard spheres with a continuous or discrete size distribution were previously obtained [68,97]. We collect these results here to show that when each subpacking associated with each component is hyperuniform, the entire packing is hyperuniform, which has been termed *multihyperuniformity* in the case of a point configuration [43]. (The Supplemental Material collects analogous expressions for $\chi_v(\mathbf{r})$ and $\tilde{\chi}_v(\mathbf{k})$ [98].)

In the case of a continuous distribution in radius, $\mathcal{R}$ is characterized by a probability density function $f(\mathcal{R})$ that normalizes to unity,

$$\int_0^\infty f(\mathcal{R}) d\mathcal{R} = 1. \tag{A1}$$

Let us denote the size average of a function $G(\mathcal{R})$ by

$$\langle G(\mathcal{R}) \rangle_{\mathcal{R}} \equiv \int_0^\infty f(\mathcal{R}) G(\mathcal{R}) d\mathcal{R}. \tag{A2}$$

The specific surface and the autocovariance function are given, respectively, by

$$s = \rho \langle s_1(\mathcal{R}) \rangle_{\mathcal{R}} \tag{A3}$$

and

$$\chi_s(\mathbf{r}) = \rho \langle m_s(r;\mathcal{R}) \otimes m_s(r;\mathcal{R}) \rangle_{\mathcal{R}} \\ + \rho^2 \langle \langle m_s(r;\mathcal{R}_1) \otimes m_s(r;\mathcal{R}_2) \otimes h(\mathbf{r};\mathcal{R}_1,\mathcal{R}_2) \rangle_{\mathcal{R}_1} \rangle_{\mathcal{R}_2}, \tag{A4}$$

where $h(\mathbf{r};\mathcal{R}_1,\mathcal{R}_2)$ is the appropriate generalization of the total correlation function for the centers of two spheres of radii $\mathcal{R}_1$ and $\mathcal{R}_2$ separated by a distance r. Note that generally h is not symmetric with respect to interchange of the components, i.e., $h(\mathbf{r};\mathcal{R}_1,\mathcal{R}_2) \neq h(\mathbf{r};\mathcal{R}_2,\mathcal{R}_1)$. Fourier transformation of (A4) gives the corresponding surface-area spectral density

$$\tilde{\chi}_s(\mathbf{k}) = \rho \langle \tilde{m}_s^2(k;\mathcal{R}) S(\mathbf{k};\mathcal{R}) \rangle_{\mathcal{R}} \\ + \rho^2 \langle \langle \tilde{m}_s(k;\mathcal{R}_1) \tilde{m}_s(k;\mathcal{R}_2) \tilde{h}(\mathbf{k};\mathcal{R}_1,\mathcal{R}_2) \rangle_{\mathcal{R}_1} \rangle_{\mathcal{R}_2} \\ - \rho^2 \langle \tilde{m}_s^2(k;\mathcal{R}) \tilde{h}(\mathbf{k};\mathcal{R}) \rangle_{\mathcal{R}}, \tag{A5}$$

where

$$S(\mathbf{k};\mathcal{R}) = 1 + \rho \tilde{h}(\mathbf{k};\mathcal{R}) \tag{A6}$$

is the non-negative structure factor for particles of radius $\mathcal{R}$. While the first term on the right side of relation (A5) must be non-negative for all $\mathbf{k}$, the remaining two terms together can be negative for some $\mathbf{k}$. The hyperuniformity condition is obtained by evaluating (A5) and setting it equal to zero [133]; i.e.,

$$\tilde{\chi}_s(\mathbf{0}) = 0 = \rho \langle s^2(\mathcal{R}) S(\mathbf{0};\mathcal{R}) \rangle_{\mathcal{R}} \\ + \rho^2 \langle \langle s(\mathcal{R}_1) s(\mathcal{R}_2) \tilde{h}(\mathbf{0};\mathcal{R}_1,\mathcal{R}_2) \rangle_{\mathcal{R}_1} \rangle_{\mathcal{R}_2} \\ - \rho^2 \langle s^2(\mathcal{R}) \tilde{h}(\mathbf{0};\mathcal{R}) \rangle_{\mathcal{R}}. \tag{A7}$$

One can obtain corresponding results for spheres with M different radii, $a_1, a_2, \ldots, a_M$, from the continuous case

[68,134] by letting

$$f(R) = \sum_{i=1}^{M} \frac{\rho_i}{\rho} \delta(\mathcal{R} - a_i), \quad (A8)$$

where ρ_i is the number density of type-i particles, respectively, and ρ is the *total number density*. Thus, from the relations above and (A8),

$$s = \sum_{i=1}^{M} \rho_i s_1(a_i), \quad (A9)$$

$$\chi_s(\mathbf{r}) = \sum_{i=1}^{M} \rho_i v_2^{int}(r; a_i)$$
$$+ \sum_{i=1}^{M} \sum_{j=1}^{M} \rho_i \rho_j \, m_s(r; a_i) \otimes m_s(r; a_j) \otimes h(\mathbf{r}; a_i, a_j), \quad (A10)$$

and

$$\tilde{\chi}_s(\mathbf{k}) = \sum_{i=1}^{M} \rho_i \tilde{m}_s^2(k; a_i) S(\mathbf{k}; a_i)$$
$$+ \sum_{i \neq j}^{M} \rho_i \rho_j \, \tilde{m}_s(k; a_i) \tilde{m}_s(k; a_j) \tilde{h}(\mathbf{k}; a_i, a_j). \quad (A11)$$

It immediately follows that at the origin $\mathbf{k} = \mathbf{0}$ we have

$$\tilde{\chi}_s(\mathbf{0}) = \sum_{i=1}^{M} \rho_i s^2(a_i) S(\mathbf{0}; a_i)$$
$$+ \sum_{i \neq j}^{M} \rho_i \rho_j \, s(a_i) s(a_j) \tilde{h}(\mathbf{0}; a_i, a_j). \quad (A12)$$

When the spatial patterns associated with each component of a polydisperse packing are themselves hyperuniform [i.e., the first term on the right side of (A12) is zero], it follows that the second term must be identically zero, and hence the polydisperse packing is multihyperuniform with respect to surface-area fluctuations. The proof follows in exactly the same way as for multihyperuniformity of polydisperse sphere packings with respect to volume-fraction fluctuations [91] and hence is not presented here explicitly.

Note that any decoration of a crystal in which each component is arranged in a periodic fashion is multihyperuniform. By contrast, constructing disordered multihyperuniform polydisperse packings is considerably more challenging. The photoreceptor mosaics in avian retina are such examples offered by nature [43].

Examining the structure factor $S(\mathbf{k})$ of the point configurations derived from the centers of spheres in a polydisperse packing could lead one to incorrectly conclude that the packing is not hyperuniform. One way to ascertain hyperuniformity in this case is through a packing's phase spectral density $\tilde{\chi}_V(\mathbf{k})$ [28,31,72,73]. Another way is through surface-area spectral density $\tilde{\chi}_s(\mathbf{k})$ via the equations given in this appendix.

[1] B. Widom, Equation of state in the neighborhood of the critical point, J. Chem. Phys. **43**, 3898 (1965).

[2] L. P. Kadanoff, Scaling laws for Ising models near T_c, Physics **2**, 263 (1966).

[3] M. E. Fisher, The theory of equilibrium critical phenomena, Rep. Prog. Phys. **30**, 615 (1967).

[4] K. G. Wilson and J. Kogut, The renormalization group and the ϵ expansion, Phys. Rep. **12**, 75 (1974).

[5] P. J. E. Peebles, *Principles of Physical Cosmology* (Princeton University Press, Princeton, NJ, 1993).

[6] S. Warr and J.-P. Hansen, Relaxation of local density fluctuations in a fluidized granular medium, Europhys. Lett. **36**, 589 (1996).

[7] P. R. ten Wolde and D. Frenkel, Enhancement of protein crystal nucleation by critical density fluctuations, Science **277**, 1975 (1997).

[8] E. R. Nowak, J. B. Knight, E. Ben-Naim, H. M. Jaeger, and S. R. Nagel, Density fluctuations in vibrated granular materials, Phys. Rev. E **57**, 1971 (1998).

[9] A. M. Kulkarni, A. P. Chatterjee, K. S. Schweizer, and C. F. Zukoski, Depletion Interactions in the Protein Limit: Effects of Polymer Density Fluctuations, Phys. Rev. Lett. **83**, 4554 (1999).

[10] K. Lum, D. Chandler, and J. D. Weeks, Hydrophobicity at small and large length scales, J. Phys. Chem. B **103**, 4570 (1999).

[11] A. Gabrielli, F. Sylos Labini, M. Joyce, and L. Pietronero, *Statistical Physics for Cosmic Structures* (Springer-Verlag, New York, 2005).

[12] R. Chang and A. Yethiraj, Strongly charged flexible polyelectrolytes in poor solvents: Molecular dynamics simulations with explicit solvent, J. Chem. Phys. **118**, 6634 (2003).

[13] Z. Ou and M. Muthukumar, Entropy and enthalpy of polyelectrolyte complexation: Langevin dynamics simulations, J. Chem. Phys. **124**, 154902 (2006).

[14] L. Berthier, G. Biroli, J.-P. Bouchaud, W. Kob, K. Miyazaki, and D. R. Reichman, Spontaneous and induced dynamic fluctuations in glass formers. I. General results and dependence on ensemble and dynamics, J. Chem. Phys. **126**, 184503 (2007).

[15] Y. Jiao, H. Berman, T.-R. Kiehl, and S. Torquato, Spatial organization and correlations of cell nuclei in brain tumors, PLoS ONE **6**, e27323 (2011).

[16] S. Torquato and F. H. Stillinger, Local density fluctuations, hyperuniform systems, and order metrics, Phys. Rev. E **68**, 041113 (2003).

[17] J. P. Hansen and I. R. McDonald, *Theory of Simple Liquids* (Academic Press, New York, 1986).

[18] C. E. Zachary and S. Torquato, Hyperuniformity in point patterns and two-phase heterogeneous media, J. Stat. Mech.: Theory Exp. (2009) P12015.

[19] C. E. Zachary and S. Torquato, Anomalous local coordination, density fluctuations, and void statistics in disordered hyperuniform many-particle ground states, Phys. Rev. E **83**, 051133 (2011).

[20] S. Torquato, G. Zhang, and F. H. Stillinger, Ensemble Theory for Stealthy Hyperuniform Disordered Ground States, Phys. Rev. X **5**, 021020 (2015).

[21] O. U. Uche, F. H. Stillinger, and S. Torquato, Constraints on collective density variables: Two dimensions, Phys. Rev. E **70**, 046122 (2004).

[22] R. D. Batten, F. H. Stillinger, and S. Torquato, Classical disordered ground states: Super-ideal gases, and stealth and equi-luminous materials, J. Appl. Phys. **104**, 033504 (2008); Novel Low-Temperature Behavior in Classical Many-Particle Systems, Phys. Rev. Lett. **103**, 050602 (2009).

[23] J. L. Lebowitz, Charge fluctuations in Coulomb systems, Phys. Rev. A **27**, 1491 (1983).

[24] A. Gabrielli, M. Joyce, and F. Sylos Labini, Glass-like universe: Real-space correlation properties of standard cosmological models, Phys. Rev. D **65**, 083523 (2002).

[25] G. Zhang, F. Stillinger, and S. Torquato, Ground states of stealthy hyperuniform potentials. I. Entropically favored configurations, Phys. Rev. E **92**, 022119 (2015).

[26] G. Zhang, F. Stillinger, and S. Torquato, Ground states of stealthy hyperuniform potentials: II. Stacked-slider phases, Phys. Rev. E **92**, 022120 (2015).

[27] A. Donev, F. H. Stillinger, and S. Torquato, Unexpected Density Fluctuations in Disordered Jammed Hard-Sphere Packings, Phys. Rev. Lett. **95**, 090604 (2005).

[28] C. E. Zachary, Y. Jiao, and S. Torquato, Hyperuniform Long-Range Correlations are a Signature of Disordered Jammed Hard-Particle Packings, Phys. Rev. Lett. **106**, 178001 (2011).

[29] Y. Jiao and S. Torquato, Maximally random jammed packings of Platonic solids: Hyperuniform long-range correlations and isostaticity, Phys. Rev. E **84**, 041309 (2011).

[30] D. Chen, Y. Jiao, and S. Torquato, Equilibrium phase behavior and maximally random jammed state of truncated tetrahedra, J. Phys. Chem. B **118**, 7981 (2014).

[31] L. Berthier, P. Chaudhuri, C. Coulais, O. Dauchot, and P. Sollich, Suppressed Compressibility at Large Scale in Jammed Packings of Size-Disperse Spheres, Phys. Rev. Lett. **106**, 120601 (2011).

[32] R. Kurita and E. R. Weeks, Incompressibility of polydisperse random-close-packed colloidal particles, Phys. Rev. E **84**, 030401 (2011).

[33] G. L. Hunter and E. R. Weeks, The physics of the colloidal glass transition, Rep. Prog. Phys. **75**, 066501 (2012).

[34] R. Dreyfus, Y. Xu, T. Still, L. A. Hough, A. G. Yodh, and S. Torquato, Diagnosing hyperuniformity in two-dimensional, disordered, jammed packings of soft spheres, Phys. Rev. E **91**, 012302 (2015).

[35] I. Lesanovsky and J. P. Garrahan, Out-of-equilibrium structures in strongly interacting Rydberg gases with dissipation, Phys. Rev. A **90**, 011603 (2014).

[36] M. Florescu, S. Torquato, and P. J. Steinhardt, Designer disordered materials with large complete photonic band gaps, Proc. Natl. Acad. Sci. USA **106**, 20658 (2009).

[37] D. Hexner and D. Levine, Hyperuniformity of Critical Absorbing States, Phys. Rev. Lett. **114**, 110602 (2015).

[38] R. L. Jack, I. R. Thompson, and P. Sollich, Hyperuniformity and Phase Separation in Biased Ensembles of Trajectories for Diffusive Systems, Phys. Rev. Lett. **114**, 060601 (2015).

[39] J. H. Weijs, R. Jeanneret, R. Dreyfus, and D. Bartolo, Emergent Hyperuniformity in Periodically Driven Emulsions, Phys. Rev. Lett. **115**, 108301 (2015).

[40] E. Tjhung and L. Berthier, Hyperuniform Density Fluctuations and Diverging Dynamic Correlations in Periodically Driven Colloidal Suspensions, Phys. Rev. Lett. **114**, 148301 (2015).

[41] K. J. Schrenk and D. Frenkel, Communication: Evidence for non-ergodicity in quiescent states of periodically sheared suspensions, J. Chem. Phys. **143**, 241103 (2015).

[42] R. Dickman and S. D. da Cunha, Particle-density fluctuations and universality in the conserved stochastic sandpile, Phys. Rev. E **92**, 020104 (2015).

[43] Y. Jiao, T. Lau, H. Hatzikirou, M. Meyer-Hermann, J. C. Corbo, and S. Torquato, Avian photoreceptor patterns represent a disordered hyperuniform solution to a multiscale packing problem, Phys. Rev. E **89**, 022721 (2014).

[44] L. M. Burcaw, E. Fieremans, and D. S. Novikov, Mesoscopic structure of neuronal tracts from time-dependent diffusion, NeuroImage **114**, 18 (2015).

[45] A. Mayer, V. Balasubramanian, T. Mora, and A. M. Walcza, How a well-adapted immune system is organized, Proc. Natl. Acad. Sci. USA **112**, 5950 (2015).

[46] S. Torquato, A. Scardicchio, and C. E. Zachary, Point processes in arbitrary dimension from Fermionic gases, random matrix theory, and number theory, J. Stat. Mech.: Theory Exp. (2008) P11019.

[47] R. P. Feynman and M. Cohen, Energy spectrum of the excitations in liquid helium, Phys. Rev. **102**, 1189 (1956).

[48] O. Leseur, R. Pierrat, and R. Carminati, High-density hyperuniform materials can be transparent, Optica **3**, 763 (2016).

[49] S. Yu, X. Piao, J. Hong, and N. Park, Bloch-like wave dynamics in disordered potentials based on supersymmetry, Nat. Commun. **6**, 8269 (2015).

[50] É. Marcotte, F. H. Stillinger, and S. Torquato, Nonequilibrium static growing length scales in supercooled liquids on approaching the glass transition, J. Chem. Phys. **138**, 12A508 (2013).

[51] A. Coniglio and T. Aste, Cell theory for glass-forming materials and jamming matter, combining free volume and cooperative rearranging regions, arXiv:1505.05540.

[52] V. Lubchenko and P. G. Wolynes, Theory of structural glasses and supercooled liquids, Annu. Rev. Phys. Chem. **58**, 235 (2007).

[53] K. S. Schweizer, Dynamical fluctuation effects in glassy colloidal suspensions, Curr. Opin. Colloid Interface Sci. **12**, 297 (2007).

[54] S. Karmakar, C. Dasgupta, and S. Sastry, Growing length and time scales in glass-forming liquids, Proc. Natl. Acad. Sci. USA **106**, 3675 (2009).

[55] D. Chandler and J. P. Garrahan, Dynamics on the way to forming glass: Bubbles in space-time, Annu. Rev. Phys. Chem. **61**, 191 (2010).

[56] G. M. Hocky, T. E. Markland, and D. R. Reichman, Growing Point-To-Set Length Scale Correlates with Growing Relaxation Times in Model Supercooled Liquids, Phys. Rev. Lett. **108**, 225506 (2012).

[57] H. L. Montgomery, The pair correlation of zeros of the zeta function, in Proc. Symp. Pure Math. 181 (1973).

[58] F. J. Dyson, Statistical theory of the energy levels of complex systems. I, J. Math. Phys. **3**, 140 (1962).

[59] W. Man, M. Florescu, K. Matsuyama, P. Yadak, G. Nahal, S. Hashemizad, E. Williamson, P. Steinhardt, S. Torquato, and P. Chaikin, Photonic band gap in isotropic hyperuniform disordered solids with low dielectric contrast, Opt. Express **21**, 19972 (2013).

[60] W. Man, M. Florescu, E. P. Williamson, Y. He, S. R. Hashemizad, B. Y. C. Leung, D. R. Liner, S. Torquato, P. M. Chaikin, and P. J. Steinhardt, Isotropic band gaps and freeform waveguides observed in hyperuniform disordered photonic solids, Proc. Natl. Acad. Sci. USA **110**, 15886 (2013).

[61] J. Haberko, N. Muller, and F. Scheffold, Direct laser writing of three dimensional network structures as templates for disordered photonic materials, Phys. Rev. A **88**, 043822 (2013).

[62] C. De Rosa, F. Auriemma, C. Diletto, R. Di Girolamo, A. Malafronte, P. Morvillo, G. Zito, G. Rusciano, G. Pesce, and A. Sasso, Toward hyperuniform disordered plasmonic nanostructures for reproducible surface-enhanced Raman spectroscopy, Phys. Chem. Chem. Phys. **17**, 8061 (2015).

[63] R. Degl'Innocenti, Y. D. Shah, L. Masini, A. Ronzani, A. Pitanti, Y. Ren, D. S. Jessop, A. Tredicucci, H. E. Beere, and D. A. Ritchie, THz quantum cascade lasers based on a hyperuniform design, Proc. SPIE **9370**, 93700A (2015).

[64] G. Zito, G. Rusciano, G. Pesce, A. Malafronte, R. Di Girolamo, G. Ausanio, A. Vecchione, and A. Sasso, Nanoscale engineering of two-dimensional disordered hyperuniform block-copolymer assemblies, Phys. Rev. E **92**, 050601 (2015).

[65] M. Hejna, P. J. Steinhardt, and S. Torquato, Nearly hyperuniform network models of amorphous silicon, Phys. Rev. B **87**, 245204 (2013).

[66] R. Xie, G. G. Long, S. J. Weigand, S. C. Moss, T. Carvalho, S. Roorda, M. Hejna, S. Torquato, and P. J. Steinhardt, Hyperuniformity in amorphous silicon based on the measurement of the infinite-wavelength limit of the structure factor, Proc. Natl. Acad. Sci. USA **110**, 13250 (2013).

[67] Reference [18] provides explicit formulas for two phases, but the extension to more than two phases is very straightforward.

[68] S. Torquato, *Random Heterogeneous Materials: Microstructure and Macroscopic Properties* (Springer-Verlag, New York, 2002).

[69] B. L. Lu and S. Torquato, Local volume fraction fluctuations in heterogeneous media, J. Chem. Phys. **93**, 3452 (1990).

[70] J. Quintanilla and S. Torquato, Local volume fraction fluctuations in random media, J. Chem. Phys. **106**, 2741 (1997).

[71] Note that we have changed the earlier notation for the volume-fraction variance used in Ref. [18] from $\sigma_\tau^2(R)$ to $\sigma_V^2(R)$ to distinguish it from the surface-area variance $\sigma_S^2(R)$ introduced in the present paper.

[72] C. E. Zachary, Y. Jiao, and S. Torquato, Hyperuniformity, quasi-long-range correlations, and void-space constraints in maximally random jammed particle packings. I. Polydisperse spheres, Phys. Rev. E **83**, 051308 (2011).

[73] C. E. Zachary, Y. Jiao, and S. Torquato, Hyperuniformity, quasi-long-range correlations, and void-space constraints in maximally random jammed particle packings. II. Anisotropy in particle shape, Phys. Rev. E **83**, 051309 (2011).

[74] D. Chen and S. Torquato, Confined disordered strictly jammed binary sphere packings, Phys. Rev. E **92**, 062207 (2015).

[75] R. A. DiStasio, G. Zhang, F. H. Stillinger, and S. Torquato, Rational design of stealthy hyperuniform patterns with tunable order (unpublished).

[76] S. Torquato and F. H. Stillinger, New conjectural lower bounds on the optimal density of sphere packings, Exp. Math. **15**, 307 (2006).

[77] P. Debye and A. M. Bueche, Scattering by an inhomogeneous solid, J. Appl. Phys. **20**, 518 (1949).

[78] P. Debye, H. R. Anderson, and H. Brumberger, Scattering by an inhomogeneous solid. II. The correlation function and its applications, J. Appl. Phys. **28**, 679 (1957).

[79] S. Torquato and G. Stell, Microstructure of two-phase random media: I. The n-point probability functions, J. Chem. Phys. **77**, 2071 (1982).

[80] S. Torquato and G. Stell, Microstructure of two-phase random media. II. The Mayer-Montroll and Kirkwood-Salsburg hierarchies, J. Chem. Phys. **78**, 3262 (1983).

[81] S. Torquato, Effective electrical conductivity of two-phase disordered composite media, J. Appl. Phys. **58**, 3790 (1985).

[82] J. G. Berryman and G. W. Milton, Normalization constraint for variational bounds on fluid permeability, J. Chem. Phys. **83**, 754 (1985).

[83] J. G. Berryman and G. W. Milton, Microgeometry of random composites and porous media, J. Phys. D: Appl. Phys. **21**, 87 (1988).

[84] A. K. Sen and S. Torquato, Effective conductivity of anisotropic two-phase composite media, Phys. Rev. B **39**, 4504 (1989).

[85] L. V. Gibiansky and S. Torquato, Geometrical-parameter bounds on effective moduli of composites, J. Mech. Phys. Solids **43**, 1587 (1995).

[86] G. W. Milton, *The Theory of Composites* (Cambridge University Press, Cambridge, UK, 2002).

[87] D. C. Pham and S. Torquato, Strong-contrast expansions and approximations for the effective conductivity of isotropic multiphase composites, J. Appl. Phys. **94**, 6591 (2003).

[88] S. Torquato and D. C. Pham, Optimal Bounds on the Trapping Constant and Permeability of Porous Media, Phys. Rev. Lett. **92**, 255505 (2004).

[89] S. Torquato, Exact Expression for the Effective Elastic Tensor of Disordered Composites, Phys. Rev. Lett. **79**, 681 (1997).

[90] M. C. Rechtsman and S. Torquato, Effective dielectric tensor for electromagnetic wave propagation in random media, J. Appl. Phys. **103**, 084901 (2008).

[91] S. Torquato, Disordered hyperuniform heterogeneous materials, J. Phys.: Condens. Matter **28**, 414012 (2016).

[92] M. Doi, A new variational approach to the diffusion and the flow problem in porous media, J. Phys. Soc. Jpn. **40**, 567 (1976).

[93] J. Rubinstein and S. Torquato, Diffusion-controlled reactions: Mathematical formulation, variational principles, and rigorous bounds, J. Chem. Phys. **88**, 6372 (1988).

[94] J. Rubinstein and S. Torquato, Flow in random porous media: Mathematical formulation, variational principles, and rigorous bounds, J. Fluid Mech. **206**, 25 (1989).

[95] S. Torquato and G. Stell, Microstructure of two-phase random media. V. The n-point matrix probability functions for impenetrable spheres, J. Chem. Phys. **82**, 980 (1985).

[96] In this paper, we denote by $m_v(r;a)$ the sphere indicator function, as opposed to the standard notation $m(r;a)$ [68,79], in order to distinguish it from the interface indicator function of a sphere, denoted by $m_s(r;a)$ here.

[97] B. L. Lu and S. Torquato, General formalism to characterize the microstructure of polydispersed random media, Phys. Rev. A **43**, 2078 (1991).

[98] See Supplemental Material at http://link.aps.org/supplemental/10.1103/PhysRevE.94.022122 for explicit formulas of the autocovariance function $\chi_V(\mathbf{r})$ and spectral density $\tilde{\chi}_V(\mathbf{k})$ of polydisperse sphere packings.

[99] J. W. Cahn and J. E. Hilliard, Free energy of a nonuniform system. I. Interfacial free energy, J. Chem. Phys. **28**, 258 (1958).

[100] J. Swift and P. C. Hohenberg, Hydrodynamic fluctuations at the convective instability, Phys. Rev. A **15**, 319 (1977).

[101] S. Torquato, Microstructure characterization and bulk properties of disordered two-phase media, J. Stat. Phys. **45**, 843 (1986).

[102] S. Torquato, Interfacial surface statistics arising in diffusion and flow problems in porous media, J. Chem. Phys. **85**, 4622 (1986).

[103] S. Torquato, Statistical description of microstructures, Annu. Rev. Mater. Res. **32**, 77 (2002).

[104] J. R. Crawford, S. Torquato, and F. H. Stillinger, Aspects of correlation function realizability, J. Chem. Phys. **119**, 7065 (2003).

[105] O. U. Uche, F. H. Stillinger, and S. Torquato, On the realizability of pair correlation functions, Phys. A (Amsterdam, Neth.) **360**, 21 (2006).

[106] S. Torquato and F. H. Stillinger, Exactly solvable disordered sphere-packing model in arbitrary-dimensional Euclidean spaces, Phys. Rev. E **73**, 031106 (2006).

[107] M. Sahimi, *Heterogeneous Materials. I. Linear Transport and Optical Properties* (Springer-Verlag, New York, 2003).

[108] G. K. Batchelor, *The Theory of Homogeneous Turbulence* (Cambridge University Press, Cambridge, UK, 1959).

[109] A. S. Monin and A. M. Yaglom, *Statistical Fluid Mechanics: Mechanics of Turbulence* (MIT Press, Cambridge, MA, 1975), Vol. 2.

[110] D. J. Pine, D. A. Weitz, P. M. Chaikin, and E. Herbolzheimer, Diffusing Wave Spectroscopy, Phys. Rev. Lett. **60**, 1134 (1988).

[111] D. S. Wiersma, The physics and applications of random lasers, Nat. Phys. **4**, 359 (2008).

[112] A. Dogariu and R. Carminati, Electromagnetic field correlations in three-dimensional speckles, Phys. Rep. **559**, 1 (2015).

[113] D. Di Battista, D. Ancora, M. Leonetti, and G. Zacharakis, From amorphous speckle pattern to reconfigurable Bessel beam via wavefront shaping, arXiv:1511.04964v1.

[114] E. Komatsu, A. Kogut, M. R. Nolta, C. L. Bennett, M. Halpern, G. Hinshaw, N. Jarosik, M. Limon, S. S. Meyer, L. Page, D. N. Spergel, G. S. Tucker, L. Verde, E. Wollack, and E. L. Wright, First-year Wilkinson microwave anisotropy probe (WMAP) observations: Tests of Gaussianity, Astrophys. J. Suppl. Ser. **148**, 119 (2003).

[115] R. Blumenfeld and S. Torquato, Coarse-graining procedure to generate and analyze heterogeneous materials—Theory, Phys. Rev. E **48**, 4492 (1993).

[116] N. F. Berk, Scattering Properties of a Model Bicontinuous Structure with a Well Defined Length Scale, Phys. Rev. Lett. **58**, 2718 (1987).

[117] N. F. Berk, Scattering properties of the leveled-wave model of random morphologies, Phys. Rev. A **44**, 5069 (1991).

[118] M. Teubner, Level surfaces of Gaussian random fields and microemulsions, Europhys. Lett. **14**, 403 (1991).

[119] P. A. Crossley, L. M. Schwartz, and J. R. Banavar, Image-based models of porous media–Application to Vycor glass and carbonate rocks, Appl. Phys. Lett. **59**, 3553 (1991).

[120] A. P. Roberts and M. Teubner, Transport properties of heterogeneous materials derived from Gaussian random fields: Bounds and simulation, Phys. Rev. E **51**, 4141 (1995).

[121] A. P. Roberts, Morphology and thermal conductivity of model organic aerogels, Phys. Rev. E **55**, R1286 (1997).

[122] P. G. Saffman, The large-scale structure of homogeneous turbulence, J. Fluid Mech. **27**, 581 (1967).

[123] S. Martis, É. Marcotte, F. H. Stillinger, and S. Torquato, Exotic ground states of directional pair potentials via collective-density variables, J. Stat. Phys. **150**, 414 (2013).

[124] In the simplest setting, the Fourier transform of the pair potential is prescribed to be uniform with support where the structure factor is constrained to be zero. This results in a pair potential in direct space that is bounded and long ranged; see Ref. [20] and references therein.

[125] P. G. De Gennes and J. Prost, *The Physics of Liquid Crystals* (Oxford University Press, Oxford, UK, 1995).

[126] J. P. Huang, Z. W. Wang, and C. Holm, Computer simulations of the structure of colloidal ferrofluids, Phys. Rev. E **71**, 061203 (2005).

[127] J. L. Lebowitz and J. W. Perram, Correlation functions for nematic liquid crystals, Mol. Phys. **50**, 1207 (1983).

[128] F. Lado and S. Torquato, Two-point probability function for distributions of oriented hard ellipsoids, J. Chem. Phys. **93**, 5912 (1990).

[129] G. E. Schröder-Turk, W. Mickel, S. C. Kapfer, M. A. Klatt, F. M. Schaller, M. J. F. Hoffmann, N. Kleppmann, P. Armstrong, A. Inayat, D. Hug, M. Reichelsdorfer, W. Peukert, W. Schwieger, and K. Mecke, Minkowski tensor shape analysis of cellular, granular and porous structures, Adv. Mater. **23**, 2535 (2011).

[130] B. Jancovici, Exact Results for the Two-Dimensional One-Component Plasma, Phys. Rev. Lett. **46**, 386 (1981).

[131] F. H. Stillinger, Molecular distribution and elasticity in crystals, Phys. Rev. **142**, 237 (1966).

[132] E. Chertkov, R. A. DiStasio, Jr., G. Zhang, R. Car, and S. Torquato, Inverse design of disordered stealthy hyperuniform spin chains, Phys. Rev. B **93**, 064201 (2016).

[133] This assumes that the value of the spectral density $\tilde{\chi}_S(\mathbf{k})$ is independent of the direction in which the origin $\mathbf{k} = \mathbf{0}$ is approached.

[134] S. Torquato and B. Lu, Rigorous bounds on the fluid permeability: Effect of polydispersivity in grain size, Phys. Fluids A **2**, 487 (1990).